PARTICLE WORLD

Technical Papers of 3P Instruments
EDITION 23
SEPTEMBER 2022

Particle characterization in **additive manufacturing**

From **static-volumetric** measurements to **breakthrough curves** and simulations

Comprehensive nanoparticle characterization with optical and acoustic methods

Characterization of particles, powders and pores

Contents

- Particle characterization for additive manufacturing: Analysis of the key parameters particle size and shape using only one instrument 3
- Comprehensive nanoparticle characterization with optical and acoustic methods: BeNano 180 Zeta Pro vs. DT-1202 8
- Comprehensive analysis of soils at the Laboratory for Scientific Particle Analysis (LabSPA) 16
- Invitation to the Adsorption event series and review of our Adsorption Week 2022 21
- Investigation of Industrial Adsorbents for Carbon Capture by Gas Flow Methods 23
- New partnership for capillary flow porometers – 3P Instruments and Poretech 28
- Service for instruments from Cilas, Quantachrome, Altamira and our current product range 30

Imprint

Editor:
3P Instruments GmbH & Co. KG
Rudolf-Diesel-Straße 12
85235 Odelzhausen | Germany
Tel. +49 8134 9324 0
info@3P-instruments.de
www.3P-instruments.de

Editorial staff:
Dr. Denise Schneider

Illustrations:
3P Instruments, Infinite4Media, Adobe Stock, unsplash

ISSN 2750-7084 (Print)
ISSN 2750-7092 (Online)

Dear Readers,

Particle World 23 is here – with new experiences and results from the field of characterization of powders, particles and pores. Since we are continuously gaining new international readers, we would like to briefly introduce ourselves again. The company name 3P Instruments originated from what we do best: characterization of powders, particles and pores. With over 30 years of company experience, we can help many users of particle measurement technology in these fields. In recent years, our scope of activities has become more and more comprehensive as we have established cooperation with many international partners. Our partners and customers benefit from our LabSPA (Lab for Scientific Particle Analysis), our excellent technical service, the scientific cooperation in projects and our events and presentations. Since this year, we are again present at trade fairs and conferences, in parallel we offer online events and just started a webinar series on surface and pore analysis by adsorption. We are very much looking forward to your participation, more information and registration is available here: www.3P-instruments.com/events/

A special series of measuring instruments has been released by our partner Bettersize Instruments this year and we are very pleased to offer the BeNano series as the latest generation for particle size and zeta potential determination of nanoparticles. On page 8, you can find theoretical basics and results, but especially the comparison of the optical method with an acoustic method. Advantages and possibilities of both methods are compared for the optimal application areas. Simply request information on the BeNano at info@3P-instruments.com, we will put you in contact with the Bettersize partner in your country and assist with test measurements and instrument demonstrations.

If you are dealing with coarser powders, our article on the next page introduces you to the advantages of using a single analyzer to determine particle size distribution and perform particle shape analysis in combination. The Bettersizer S3 Plus is becoming more and more popular for such tasks, both in R&D and in quality control, e.g. in the field of additive manufacturing. Our article "Comprehensive particle and surface studies of soils" also illustrates the possibilities of the Bettersizer S3 Plus, but also exemplifies the application of other analysis methods for powder characterization.

I would also like to refer you to our webinar series on gas adsorption. 3P Instruments is continuously expanding its training opportunities in the field of surface determination and macro-, meso-, and micropore characterization. Our gas sorption webinar series open up an uncomplicated exchange of experiences - free of charge! More information can be found on page 21.

Enjoy reading the Particle World 23 and all the best for you!

Dr. Dietmar Klank

Particle characterization for additive manufacturing: Analysis of the key parameters particle size and shape using only one instrument

Dr. Frederik Schleife, frederik.schleife@3P-instruments.com
Dr. Christian Oetzel, christian.oetzel@3P-instruments.com

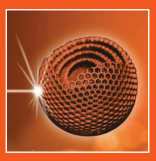

Introduction and objectives

Additive manufacturing (AM) processes can be used to produce very complex components in a precise and customized manner. Compared to conventional manufacturing processes, in which components are produced by removing excess material (top-down approach, e.g., turning, milling, grinding), additive manufacturing uses the so-called bottom-up approach. In this case, the desired workpieces are built up three-dimensionally layer by layer. This can be achieved in various ways, such as selective melting or sintering of a powder using laser or electron beams, extrusion and deposition of heated polymers or selective curing of photoactive polymers. Regardless of the selected method, additive manufacturing can be used to realize structures that would not be possible using traditional material removal processes. Another decisive advantage of AM processes lies in the short manufacturing chain between digital design and finished workpiece [1]. The information for manufacturing a specific workpiece is imported into the manufacturing machines as digital file. This allows the same component to be manufactured at different locations without any problems, even with tight specifications, since only the production machine, the digital information on the workpiece, and the raw material are required. This eliminates the need for supply chains of, for example, preliminary stages or finished workpieces, which contributes to time-efficient and more cost-effective production.

The final product properties of workpieces manufactured by means of additive manufacturing are essentially influenced by the starting material and its powder properties [2]. The most important characteristics are particle size distribution [3], particle shape [3] [4], chemical composition [5] [6], flowability [7] powder layer density (PLD) [8] [9], and internal porosity [3]. Nevertheless, there are currently no quantified or specified and widely accepted parameters for describing powder properties for the use in additive manufacturing [4], or they are kept secret by powder manufacturers for competitive reasons [2]. Thus, the monitoring of raw material quality is more than essential for additive manufacturing to ensure consistent product properties.

Another interesting correlation between the influence of powder characteristics on the final properties of the workpiece produced, for example, by laser beam melting (LBM - Laser Beam Melting/ SLM - Selective Laser Melting) arises from the question of whether powder fed into the process but not melted must be discarded or can be reused for production [10]. Since the production volume of components manufactured by laser melting is continuously increasing [11] and the majority of the powder used (95-97 % [12]) is not melted, this question should be answered from both economic and ecological aspects.

During the LBM process, so-called spatter particles are formed, which are deposited in the powder bed and in the production zone of the LBM machine and thus accumulate in the recycling powder [13]. It is also known that a higher energy density of the laser radiation used leads to an increase in the formation of spatter particles [14] [15].

Although the influence of the spatter particles on the final product quality of the manufactured workpiece needs to be further investigated, the analysis of the particle size distribution and particle shape of the fresh powder compared to the spatter particles is a crucial approach [10].

In addition to the classical method of laser diffraction (static laser light scattering) for the determination of the particle size distribution, an imaging method is needed for the acquisition of the shape factors of particle collectives and especially of single particles. In this context, dynamic image analysis is excellent in providing statistics and thus representative analysis of the mean particle shape parameters of the entire collective due to the rapid capture of many individual particles. In addition, single particle acquisition allows the detection and analysis of statistically underrepresented oversized particles or fractions of heterogeneous powder samples with respect to size and/or shape.

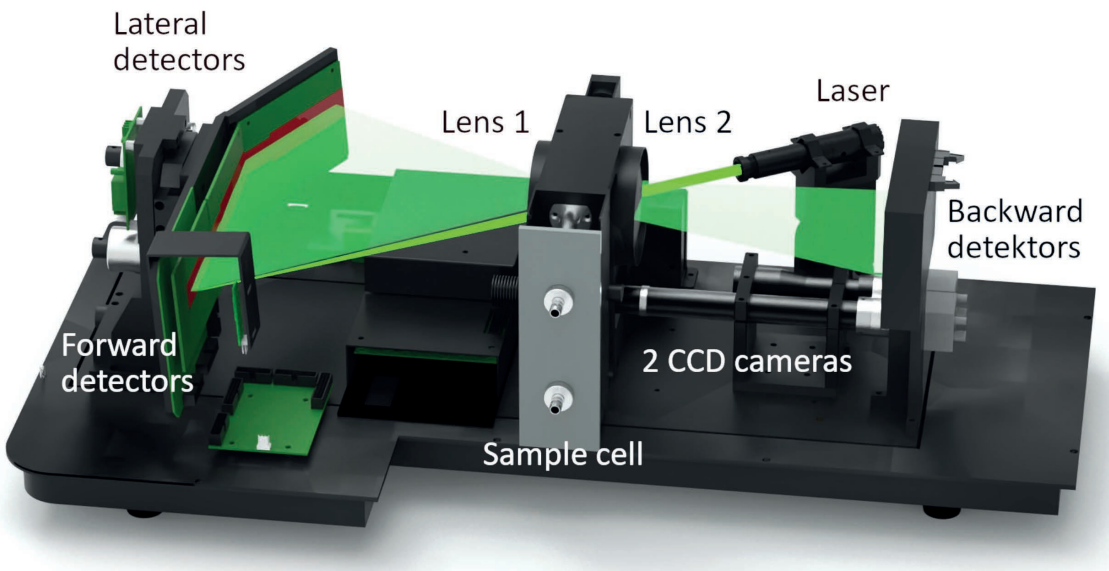

Figure 1 *Setup of the Bettersizer S3 Plus incl. dual lens system with DLOI (Dual Lenses & Oblique Incidence) system and CCD camera unit (0.5x and 10x)*

The Bettersizer S3 Plus is a measuring instrument that uniquely allows the analysis of particle size distribution from the nano to the millimeter range by means of classical laser diffraction and the simultaneous characterization of particle shape as well as oversize and agglomeration phenomena by means of dynamic image analysis.

The Bettersizer S3 Plus: one instrument, two essential powder properties

Fig. 1 shows the optical unit of the Bettersizer S3 Plus: the wet measuring cell is located in the center of the main platform, two Fourier lenses are placed directly to the right and left of the cell (two Fourier lenses = dual lens technology). To the right of the measuring cell is the laser light source arranged at an angle (green diode pumped solid state ((DPSS)) laser, wavelength = 532 nm), directed perpendicular to the measuring cell is the CCD camera system (two cameras with different lenses: 0.5x and 10x) and the backscattering detectors.

To the left of the measuring cell, the detector system for detecting forward and side scattering is installed. This special setup enables:

1. The exact measurement of very small particles (from 10 nm) using the double lens technique (static laser light scattering, see section 2.1).

2. At the same time, highest measuring precision for very coarse particles (up to 3.5 mm), optionally supported by the 0.5 x CCD camera (static laser light scattering combined with dynamic image analysis)

3. Particle shape determination, oversized particle analysis and agglomerate check with the 0.5 x and/or 10 x CCD camera (dynamic image analysis, see next page).

Laser diffraction/static laser light scattering with the innovative double lens technique (DLOIOS)

Fig. 1 shows the schematic diagram of the Bettersizer S3 Plus: the special feature of this laser setup is the DLOI (Dual Lenses & Oblique Incidence) system. The laser is arranged inclined to the measuring cuvette to allow the widest possible scattering angle range of the lateral front detectors. Fourier lens 2 produces an exact parallel laser beam that impinges on the sample. Lens 1 focuses the scattered light into the detector plane according to the known Fourier setup, thus the scattering particles in the cuvette do not necessarily have to lie in one plane - a decisive advantage over the conventional reverse Fourier setup [16]. Lens 2, in turn, ensures focusing and thus detection of the backscattered radiation, yielding a very large angular range (0.02 - 165°) with excellent detector resolution compared to other systems on the market. In particular, a high scattered light resolution in the backscattering range (> 90°) is crucial for the accurate detection of very small particles (< approx. 500 nm) [16].

The extremely wide angular coverage also has the advantage that a second, shorter-wavelength laser can be avoided. Accordingly, no scattering spectra of mixed wavelengths are measured, which is advantageous as the evaluation of those spectra is strictly speaking not allowed using the commonly used models (Fraunhofer and Mie).

Dynamic image analysis for particle shape analysis

Depending on the distribution range of the sample to be analyzed, the two high-speed CCD cameras of the Bettersizer S3 Plus can be used either individually or in combination for comprehensive particle size and shape analysis solely based on dynamic image analysis. The according size range is

- 30 – 3,500 µm for the 0.5x camera
- 2 – 50 µm for the 10x camera

Depending on the particle size and sample concentration, several thousand to several 100,000 particles can be recorded per minute with both cameras. For very broad distributions, the combined use of both cameras is recommended.

During the analysis, each individual particle is captured in real time, stored as an image, numbered and statistically evaluated [17]. In addition to various equivalent diameters (e.g., area, perimeter, maximum and minimum Feret), special shape parameters such as aspect ratio, length L/width D, circularity (roundness), convexity, perimeter and many more are calculated [18].

Particularly in the case of strongly shape-anisotropic particles such as fibers or platelets, this is a clear advantage over classical, "pure" laser diffraction, which assumes spherical particles during evaluation. Furthermore, the degree of agglomeration of the systems can be assessed and special tasks such as oversize particle analysis can be realized. The determination of different equivalent diameters also offers the possibility to compare with other methods for size determination, such as sieving, and to verify their measurement results.

Application example: the particulate properties of a fresh AlSi10Mg powder compared to the powder recovered after the LBM process

In order to illustrate the advantages of the Bettersizer S3 Plus for the quality assessment of powder samples for additive manufacturing using an application-related example, two different AlSi10Mg samples were examined with regard to their particle size distribution and particle shape. The sample AlSi10Mg fresh was a fresh powder, as received from the supplier. This was fed to an SLM manufacturing machine. After the production step, the sample AlSi10Mg spatter particles was recovered from the fabrication zone of the SLM machine. Both powder samples were dispersed separately in ethanol and characterized using the Bettersizer S3 Plus with respect to particle size distribution by classical laser diffraction and particle shape by dynamic image analysis. For this purpose, the powder samples were added to the ethanol-filled dispersion unit of the Bettersizer S3 Plus and pretreated with the device's internal ultrasonic dispersion for one minute before measurement.

Tab. 1 shows the characteristic diameters of the volume-based particle size distributions obtained by laser diffraction. In Fig. 2, the superimposed distribution functions are shown graphically as histograms and cumulative curves.

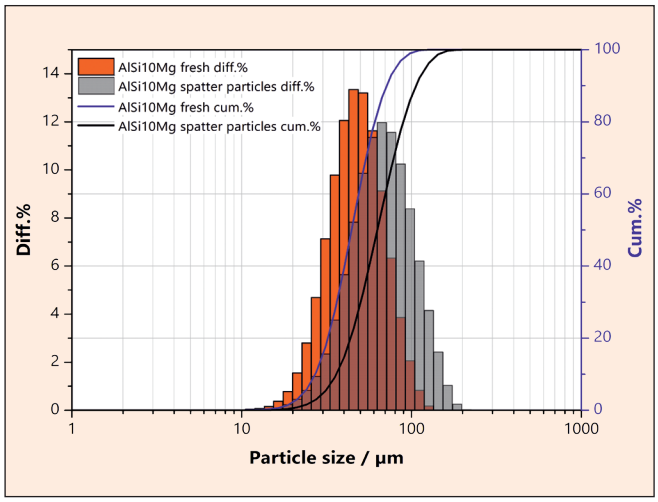

Figure 2 *Superposition of the volume-based particle size distributions of the investigated samples obtained by laser diffraction*

From the measurement results of the laser diffraction experiments, it is clear that the spatter particles have a coarser particle size distribution compared to the fresh AlSi10Mg sample. Likewise, from the SPAN values determined (=(D90-D10)/D50), it is evident that the AlSi10Mg spatter particles have a broader distribution than AlSi10Mg fresh.

Table 1 *Characteristic diameters of the volume-based particle size distributions of the investigated samples obtained by laser diffraction*

Sample	D10 / µm	D50 / µm	D90 / µm	D97 / µm	SPAN
AlSi10Mg fresh	27.08	44.39	71.10	86.72	0.991
AlSi10Mg spatter particles	36.20	62.89	106.40	131.70	1.117

For the evaluation of the particle shape, a representative number of individual particles were recorded from both samples with the high-speed CCD cameras of the Bettersizer S3 Plus and were evaluated number-based with respect to the ISO shape parameters circularity and aspect ratio. The characteristic values of the distribution functions of both shape parameters are summarized in Tab. 2 and superimposed in Fig. 3 and 4. Tab. 3 and 4 list selected individual particle parameters of the six largest particles detected with the 10x camera of the Bettersizer S3 Plus and show their appearance.

The results of the dynamic image analyses on both samples, as well as their comparison with each other, show a significantly larger aspect ratio and thus a lower average expansion of the spatter particles (sample AlSi10Mg spatter particles) compared to the particles of the unused powder sample AlSi10Mg fresh. Likewise, the spatter particles exhibit higher mean circularity and are thus characterized by lower shape anisotropy (resp. higher sphericity) than the particles before being used in the AM process.

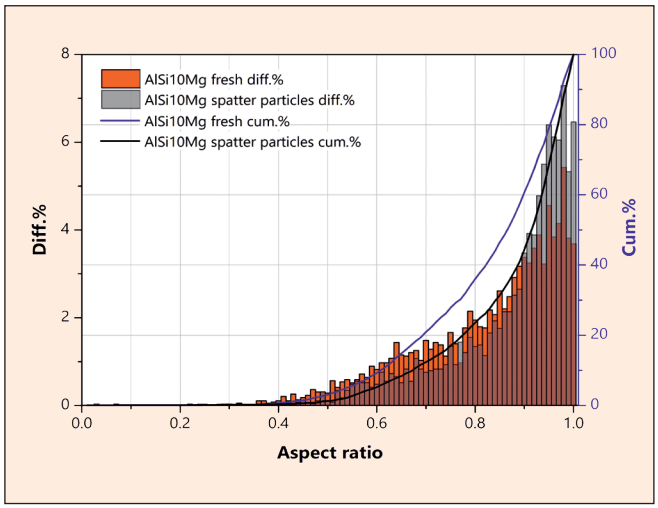

Figure 3 *Superposition of the number-based distribution functions of the aspect ratio of the studied samples*

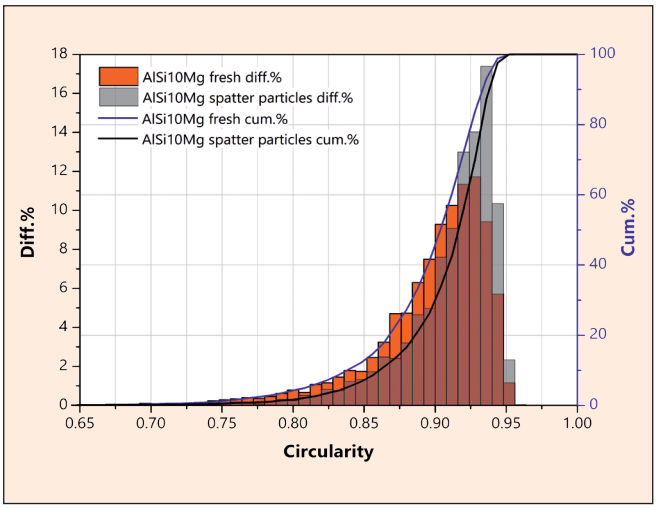

Figure 4 *Superposition of the number-based distribution functions of the circularity of the studied samples*

Table 2 *Characteristic % values of the number-based particle shape distributions of the investigated samples obtained by dynamic image analysis*

Sample	Number of detected particles	Parameter	x1	x10	x50	x90	x99
AlSi10Mg fresh	3,909	Circularity	0.739	0.839	0.904	0.933	0.945
		Aspect ratio	0.425	0.608	0.866	0.975	1.000
AlSi10Mg spatter particles	2,909	Circularity	0.782	0.861	0.917	0.938	0.947
		Aspect ratio	0.487	0.672	0.916	0.983	1.000

Table 3 *Selected single particle parameters of the 6 largest particles of the sample AlSi10Mg fresh detected by the 10x camera*

No.	Area / µm²	CE diameter / µm	Length / µm	Width / µm	Circularity	Convexity	Aspect ratio	Image
1	6,600	91.67	139.3	62.87	0.771	0.892	0.451	
2	6,069	87.91	128.7	61.40	0.801	0.920	0.476	
3	5,632	84.68	121.2	61.55	0.767	0.876	0.507	
4	5,303	82.17	105.5	71.61	0.755	0.868	0.678	
5	5,021	79.95	125.8	53.53	0.737	0.888	0.425	
6	5,017	79.92	94.1	70.70	0.833	0.885	0.751	

Table 4 Selected single particle parameters of the 6 largest particles of the sample AlSi10Mg spatter particles detected by the 10x camera

No.	Area / µm²	CE diameter / µm	Length / µm	Width / µm	Circularity	Convexity	Aspect ratio	Image
1	20,049	159.7	162.3	154.6	0.862	0.886	0.952	
2	16,984	147.0	168.7	132.1	0.912	0.938	0.783	
3	13,117	129.2	132.3	128.9	0.903	0.924	0.974	
4	11,470	120.8	122.7	116.9	0.854	0.888	0.953	
5	11,237	119.6	120.8	113.5	0.907	0.938	0.940	
6	10,863	117.6	134.0	108.0	0.835	0.871	0.805	

The results of the dynamic image analyses on both samples, as well as their comparison with each other, show a significantly larger aspect ratio and thus a lower average expansion of the spatter particles (sample AlSi10Mg spatter particles) compared to the particles of the unused powder sample AlSi10Mg fresh. Likewise, the spatter particles exhibit higher mean circularity and are thus characterized by lower shape anisotropy (resp. higher sphericity) than the particles before being used in the AM process.

Summary and conclusion

Based on the investigations carried out with the Bettersizer S3 Plus, both samples analyzed in terms of particle size and shape can be clearly distinguished from each other. The findings that the spatter particles recovered after the additive manufacturing process are characterized by a coarser and more widely distributed particle size and higher sphericity compared to the fresh AlSi10Mg particles are in line with observations known from the literature [10]. This shows that the Bettersizer S3 Plus is perfectly suitable for the quality control of raw materials for additive manufacturing processes, and also makes a significant contribution to a better understanding of the influences on the final product properties of the workpieces produced by additive manufacturing from a research and development perspective. This is essentially due to the unique combination of laser diffraction and dynamic image analysis measurement methods in one measuring device. This enables a fast, simple and cost-efficient analysis of the powder raw materials.

For the final answer to the question of whether a recovered powder is appropriate for reuse in additive manufacturing or whether it must be subjected to further preparative steps (sieving, purification, mixing with fresh powder), additional investigations are necessary. A chemical analysis of the alloy composition and an assessment of the quality of workpieces produced using recovered powder are essential.

Acknowledgement

We would like to thank Prof. Dr.-Ing. Vesna Nedeljkovic-Groha and Dipl.-Ing. Stefan Brenner of the Faculty of Mechanical Engineering at the Universität der Bundeswehr München for kindly providing the samples as well as advice and explanations on the application side.

Literature

[1] J. A. Slotwinski, E. J. Garboczi, P. E. Stutzman, C. F. Ferraris, S. S. Watson und M. A. Peltz, „Characterization of Metal Powders Used for Additive Manufacturing," Journal of Research of the National Institute of Standards and Technology, Bd. 119, p. 460, 2014.

[2] L. Haferkamp, L. Haudenschild, A. Spierings, K. Wegener, K. Riener, S. Ziegelmeier und G. J. Leichtfried, „The Influence of Particle Shape, Powder Flowability, and Powder Layer Density on Part Density in Laser Powder Bed Fusion," Metals, Bd. 11, Nr. 3, p. 418, 2021.

[3] W. J. Sames, F. A. List, S. Pannala, R. R. Dehoff und S. S. Babu, „The metallurgy and processing science of metal additive manufacturing," Int. Mater. Rev., Bd. 61, p. 315, 2016.

[4] J. H. Tan, W. L. Wong und K. W. Dalgarno, „An overview of powder granulometry on feedstock and part performance in the selective laser melting process," Addit. Manuf., Bd. 18, p. 228, 2017.

[5] R. Engeli, T. Etter, S. Hövel und K. Wegener, „Processability of different IN738LC powder batches by selective laser melting," J. Mater. Process. Technol., Bd. 229, p. 484, 2016.

[6] J. A. Slotwinski und E. J. Garboczi, „Metrology Needs for Metal Additive Manufacturing Powders," J. Mater., Bd. 67, p. 538, 2015.

[7] A. B. Spierings, M. Voegtlin, T. Bauer und K. Wegener, „Powder flowability characterisation methodology for powder-bed-based metal additive manufacturing," Prog. Addit. Manuf., Bd. 1, p. 9, 2016.

[8] T. M. Wischeropp, C. Emmelmann, M. Brandt und A. Pateras, „Measurement of actual powder layer height and packing density in a single layer in selective laser melting," Addit. Manuf., Bd. 28, p. 176, 2019.

[9] Y. Mahmoodkhani, U. Ali, S. Imani Shahabad, A. Rani Kasinathan, R. Esmaeilizadeh, A. Keshavarzkermani, E. Marzbanrad und E. Toyserkani, „On the measurement of effective powder layer thickness in laser powder-bed fusion additive manufacturing of metals," Prog. Addit. Manuf., Bd. 4, p. 109, 2019.

[10] M. Lutter-Günther, M. Bröker, T. Mayer, S. Lizak, C. Seidel und G. Reinhart, „Spatter formation during laser beam melting of AlSi10Mg and effects on powder quality," Procedia CIRP, Bd. 74, p. 33, 2018.

[11] T. Wohlers, „3D printing and additive manufacturing state of the industry: annual worldwide progress report," Wohlers Report, 2017.

[12] B. A. Hann, „Powder Reuse and Its Effects on Laser Based Powder Fusion Additive Manufactured Alloy 718," in SAE 2016 Aerospace Systems and Technology Conference, Warrendale, PA, 2016.

[13] Y. Liu, Y. Yang, S. Mai, D. Wang und C. Song, „Investigation into spatter behavior during selective laser melting of AlSi 316L stainless steel powder," Materials & Design, Bd. 87, p. 797, 2015.

[14] D. Wang, S. Wu, F. Fu, S. Mai, Y. Yang, Y. Liu und C. Song, „Mechanisms and characteristics of spatter generation in SLM processing and its effect on the properties," Material & Design, Bd. 117, p. 121, 2017.

[15] M. Taheri Andani, R. Dehghani, M. R. Karamooz-Ravari, R. Mirzaeifar und J. Ni, „A study on the effect of energy input on spatter particles creation during selective laser melting process," Addit. Manuf., Bd. 20, p. 33, 2018.

[16] ISO 13320:2020-01, Particle size analysis - Laser diffraction methods, 2020.

[17] ISO 13322-2:2006-11, Particle size analysis - Image analysis methods - Part 2: Dynamic image analysis methods, 2006.

[18] ISO 9276-6:2008-09, Representation of results of particle size analysis - Part 6: Descriptive and quantitative representation of particle shape and morphology, 2008.

Comprehensive nanoparticle characterization with optical and acoustic methods: BeNano 180 Zeta Pro vs. DT-1202

Dr. Marion Ferner, marion.ferner@3P-instruments.com
Dr. Christian Oetzel, christian.oetzel@3P-instruments.com

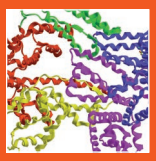

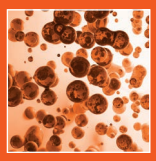

Introduction

The characterization of nanoscale particles (definition see [1]) with regard to their particle size and colloidal properties sets high demands on the used measurement technology. Due to their very small size, they can hardly be detected with standard techniques and have a very large ratio of the particle surface area to the particle volume, which often leads to strong agglomeration in liquids.

Common methods for particle size determination such as sieving, light microscopy or sedimentation are not applicable for these materials. Electron microscopic techniques on the other hand are complex, expensive and do not provide reliable statistics. In addition, there is no possibility to determine further colloidal properties such as electrical conductivity, pH value or zeta potential in combination - parameters that are often very important for development or quality control in such systems in combination with particle size distribution.

For this reason, optical and acoustic fitting methods have established on the market over time: on the "optical side", these are dynamic light scattering (DLS, [2]) in combination with electrophoretic light scattering (ELS, [3]) and static light scattering (SLS). The common acoustic systems are acoustic attenuation spectroscopy [4] and electroacoustics [5]. Optical and acoustic methods are usually not in direct competition, but the suitable method group depends on the specific application.

In the following, these techniques are presented using the commercial devices BeNano 180 Zeta Pro [6] and DT-1202 [7] as an example. In particular, their benefits but also limits will be described. At the end, the methods are compared with each other and a recommendation for the respective use is given (see Tab. 5).

Dynamic light scattering, electrophoretic light scattering and static light scattering – BeNano 180 Zeta Pro

The BeNano series is the latest generation of nanoparticle analyzers designed by Bettersize Instruments Ltd. The BeNano 180 Zeta Pro determines particle size (dynamic light scattering – DLS), zeta potential (electrophoretic light scattering - ELS) molecular weight (static light scattering - SLS) and additional parameters like time and temperature-dependent trends of particle size and zeta potential. An overview of the optical system of the BeNano 180 Zeta Pro is given in Fig. 1.

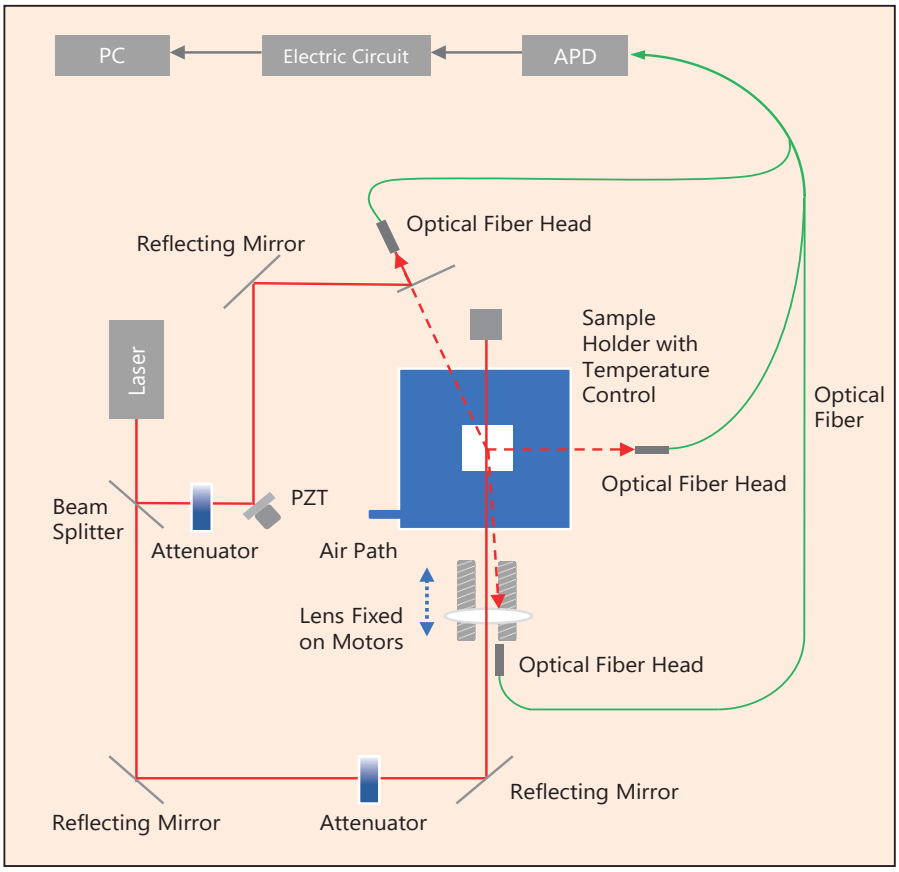

Figure 1 *Optical system of the BeNano 180 Zeta Pro*

Dynamic light scattering for size determination of nanoparticles

Dynamic light scattering (DLS) is a sizing technology measuring the diffusion behaviour of the particles dispersed in liquids. When nanoparticles are suspended in the liquid medium, the continuous random movement of the nanoparticles (Brownian motion) is related to the size of particles. The measurement principle is shown in Fig. 2: a laser light beam (in case of the BeNano 180 Zeta Pro with a wavelength of 671 nm) hits finely distributed, small particles (generally < 1 µm) in a liquid dispersion and is scattered by them. The scattered light of the particles interferes with each other. Since the particles are constantly changing their location due to Brownian motion, the position of the scattering centres change relative to one another and the interference leads to small fluctuations in the scattering intensity. The change in the scattered light intensity as a function of time is measured at a specific, fixed angle (90° or 173°) to the direction of incidence of the laser beam. This gives information about the speed of the particles in the liquid (small particles move faster than large particles), the diffusion coefficient with the help of an autocorrelation of the raw data and the particle size (hydrodynamic diameter DH) via the Stokes-Einstein relationship (Eq. 1).

$$D = \frac{k_B T}{3\pi\eta D_H} \quad (1)$$

D: diffusion coefficient
k_B: Boltzmann's constant
T: temperature
η: dynamic viscosity (medium)
D_H: hydrodynamic diameter

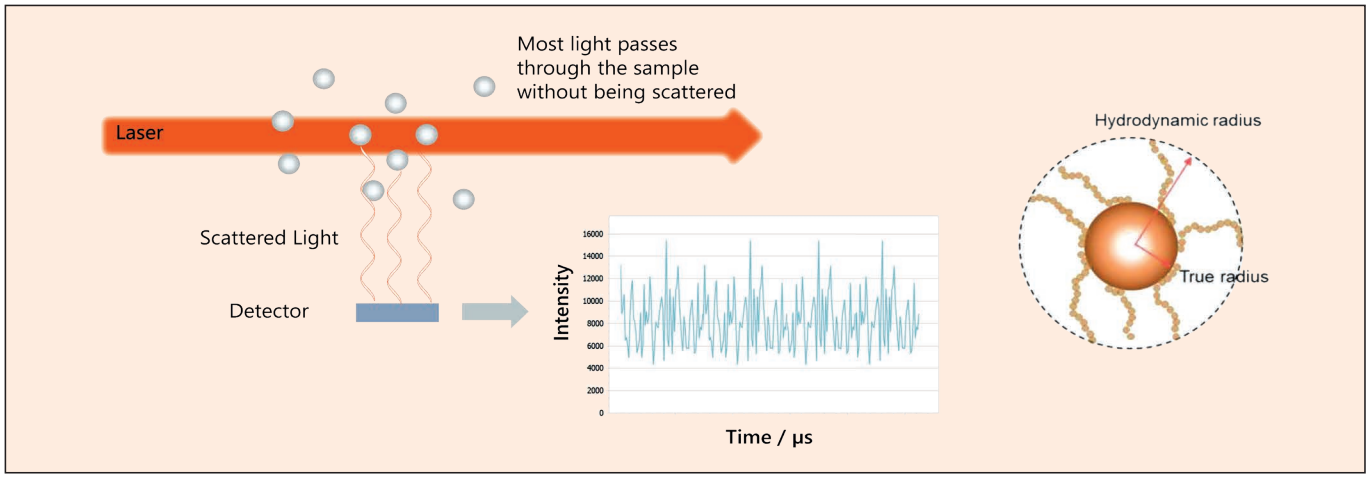

Figure 2 *Principle of dynamic light scattering*

In contrast to the classic 90° detection, the 173° backscattering detection of the BeNano 180 Zeta Pro enables measurements of highly diluted samples with weak light scattering due to greater sensitivity and, in connection with a variable detection position, particle size measurements of concentrated samples (max. 40 % (w/v), sample dependent) by eliminating multiple light scattering.

The original signal determined by DLS is weighted according to the intensity of scattered light. Particle size distributions are described by two parameters: the mean (intensity-weighted) hydrodynamic particle diameter Z-ave and the polydispersity index PDI (parameter of the distribution width). The size distribution can be calculated from the original signal using suitable algorithms (GENERAL or CONTIN).

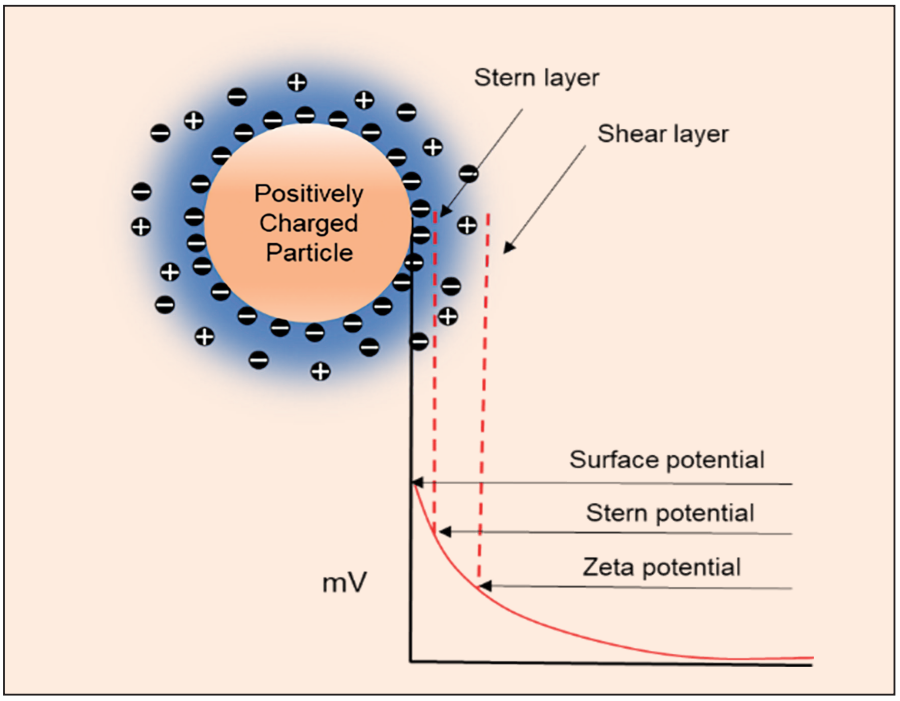

Figure 3 *Potential distribution at particle surface*

Electrophoretic light scattering for zeta potential determination of nanoparticles

Electrophoretic light scattering (ELS) is a technology for measuring electrophoretic mobility of nanoparticles using Doppler shifts of scattered light [3]. In aqueous systems, particles usually carry positive or negative charges on the surface and are surrounded by counter ions that form a firmly inner Stern layer and an outer shear layer (electro-chemical double layer). If an external force, e. g., an electric or acoustic field, is applied, the charged particles move and the diffuse layer is sheared relative to the particle and its fix connected Stern layer. The zeta potential is the electrical potential at the interface of this shear layer (Fig. 3) and is an important indicator for the stability of a particle system. At high zeta potential, the repulsive force between the particles is strong and the system tends to be stable. A low zeta potential indicates that only weak repulsive forces act between the particles, which means they tend to agglomerate or flocculate. This is then referred to as low dispersion stability. In aqueous systems, the zeta potential is mainly determined by the pH value of the dispersing medium, the ionic strength (salt concentration) and the concentration of low-molecular additives.

In an ELS experiment an electric field is applied to the dispersion to be characterized resulting in an electrophoretic movement of the dispersed charged particles. A laser light beam (wavelength 671 nm) irradiates the sample, where the scattered light is detected at a forward angle of 12°. When incident light strikes these moving particles, the frequency of the particles' scattered light differs from the incident light due to the Doppler effect. The frequency shift is measured and converted to provide the electrophoretic mobility and hence the zeta potential of a sample by Henry's equation (2).

$$\mu = \frac{2\varepsilon_r \varepsilon_0 \zeta}{3\eta} f(\kappa\alpha) \qquad (2)$$

μ: electrophoretic mobility
ε_r: relative dielectric constant
ε_0: solvent dielectric constant in a vacuum
ζ: zeta potential
η: dynamic viscosity (medium)
$f(\kappa\alpha)$: Henry function ($\kappa\alpha$ refers to the ratio between the thickness of the double layer and the particle radius)

Based on the traditional ELS technology, the PALS technology used in the BeNano 180 Zeta Pro is a further development to measure systems with low particle mobility in particular (organic solvents, solvents with very high electric conductivity etc). In this case a phase shift between reference and scattered wave is detected by applying an alternating instead of a constant voltage at the electrophoresis cell. An overview to this technology (ELS-PALS) can be found in [3].

Static light scattering for molecular weight determination of nanoparticles

Using static light scattering (SLS), the scattering intensities and from this the weight-average molecular weight (M_W) and the second virial coefficient (A_2) of macromolecules like polymers and proteins can be measured or calculated from the Rayleigh equation (3).

$$\frac{KC}{R_\theta} = \frac{1}{M_W} + 2A_2C \qquad (3)$$

K: constant related to dn/dc (refractive index increment)
C: sample concentration
θ: detection angle
R_θ: Rayleigh ratio to characterize the intensity ratio between the scattered light and the incident light
M_W: sample's weight-average molecular weight
A_2: second virial coefficient

For molecular weight measurements, scattering intensities of the sample are recorded at different concentrations at a fixed angle (90° or 173°) to the direction of incidence of the laser beam (671nm). Using the scattering intensity and the Rayleigh ratio of a known standard (such as toluene), the Rayleigh ratios of the sample at different concentrations are calculated and presented in a Debye plot. The molecular weight and second virial coefficient can then be obtained by the intercept and slope from the linear fit of the Debye plot. The measurement principle is shown in Fig. 4.

Nano-Application of dynamic, electrophoretic and static light scattering

DLS, ELS-PALS and SLS are widely applied in academic nanoparticle research and in nanoparticle manufacturing of various fields including life sciences. Proteins are complex nano scaled biomolecules, which tend to agglomerate when isolated from or manufactured outside the physiological environment because of intermolecular interactions of monomers. Particle size, zeta potential and molecular weight are key parameters for protein stability. DLS (especially due to the backscattering technology of the BeNano 180 Zeta Pro) as well as ELS and SLS are predestined for diluted (optical clear) samples and therefore for protein analysis.

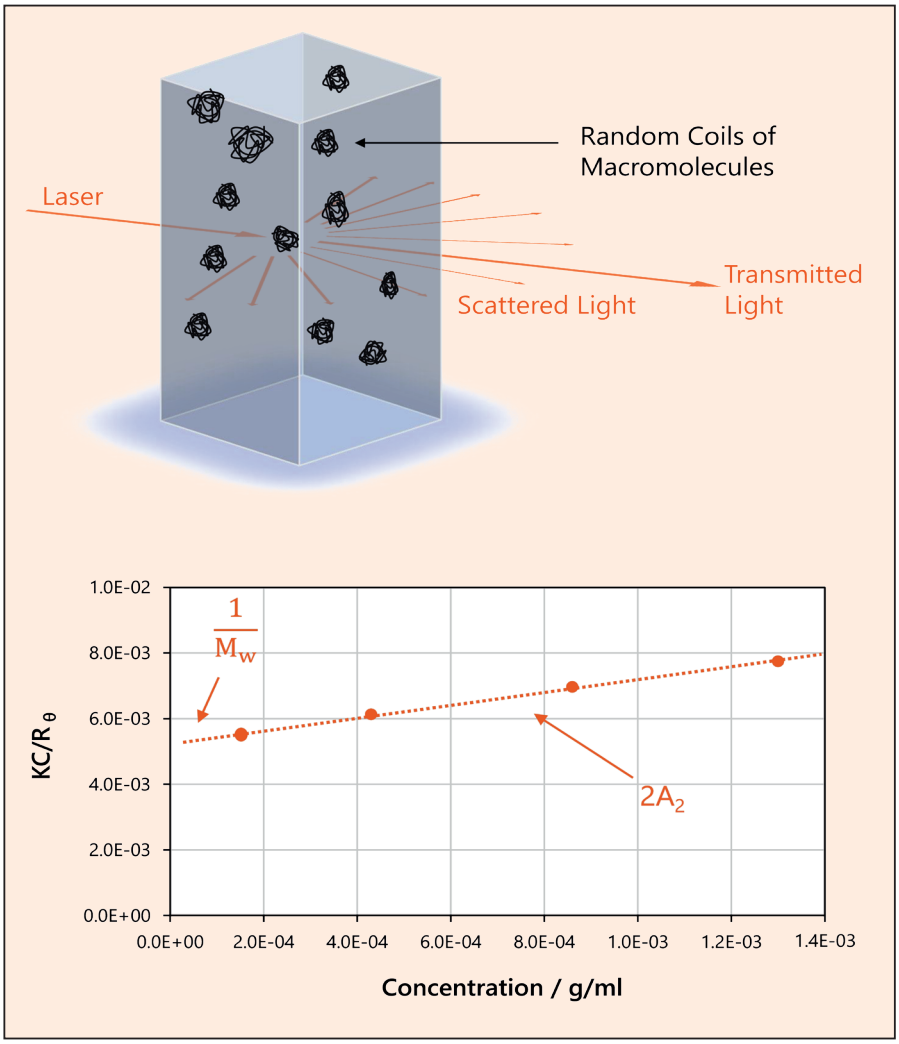

Figure 4 *Principle of static light scattering*

Bovine serum albumin (BSA) was used as model protein in the following studies by the BeNano 180 Zeta Pro. BSA (CAS No. 90604-29-8, Roth Karlsruhe) solutions (1 % w/w) were prepared in saline (0.9 % NaC w/w) or deionized water in order to investigate the dependence of protein structure and molecular interaction on the solvent environment, during ageing and at heat stress. To remove dust, both solutions were filtered with 0.2 µm filters before use.

In a first step, the size, zeta potential and molecular weight were measured to characterize BSA in different media. Differences in BSA structure are obvious in saline and water. The results are summarized in Tab. 1.

The Z-ave (mean hydrodynamic diameter) and molecular weight of BSA in saline are very close to the nominal values (size: 6,96 nm, molecular weight: 66,5 kDa) of the BSA monomer [8]. The corresponding size distribution is characterized by a single monomodal peak, indicating a homogenous monomeric particle population of BSA molecules in saline. In contrast, BSA in H_2O showed a bimodal particle size distribution, indicating different populations of BSA molecules. The smaller particle fraction corresponds to a mean particle size of 3 nm, which is much below the literature value of the BSA monomer and may indicate denaturation of BSA in H_2O. This denaturation is obvious

Table 1 *Particle size, zeta potential and molecular weight of 1% BSA in different media*

Medium	Temperature / °C	Z-ave / nm	PDI	Molecular weight / kDa	Zeta Potential / mV
Saline	25	7.92 ± 0.03	0.091 ± 0.01	87.86	-8.97 ± 0.69
H_2O	25	3.35 ± 0.03	0.302 ± 0.005	37.43	-24.06 ± 0.50

Table 2 *Particle size, zeta potential and molecular weight of 1 % BSA during ageing in saline*

Time / d	Temperature / °C	Z-ave / nm	PDI	Molecular weight / kDa	Zeta Potential / mV
0	25	7.92 ± 0.03	0.091 ± 0.010	87.86	-8.97 ± 0.69
1	25	7.87 ± 0.03	0.068 ± 0.007	90.74	-9.06 ± 0.66
2	25	8.56 ± 0.07	0.206 ± 0.012	102.22	-8.32 ± 0.46
3	25	8.90 ± 0.04	0.273 ± 0.007	104.93	-7.98 ± 0.40
6	25	9.39 ± 0.09	0.331 ± 0.012	110.18	-7.16 ± 0.20
9	25	9.22 ± 0.14	0.315 ± 0.018	102.95	-8.27 ± 0.27
14	25	10.10 ± 0.18	0.395 ± 0.013	104.01	-6.14 ± 0.21

from the lower Z-ave and the corresponding lower molecular weight compared to BSA in saline. The larger particle fraction corresponds to a mean particle size of 19,6 nm, which may characterize oligomerization of BSA molecules. Saline seems to be more advantageable in BSA studies than water because of the stabilization of BSA monomers. The lower absolute value of zeta potential of BSA in saline is due to the shielding effects of the present counter ions and is not an indicator for less BSA stability.

The stabilization of BSA in saline is obvious during ageing at 25 °C for 14 days (Tab. 2). BSA was stable for the first 24 hours of incubation. This was characterized by no changes in size, molecular weight and zeta potential of the BSA monomer. From the second day of incubation, a slight increase of Z-ave and consequently of molecular weight was detected. The reason for these changes is the presence of a second small BSA fraction during ageing which is reflected by an increasing PDI-value and may be due to the beginning aggregation of BSA. The slight decrease of zeta potential is a hint for conformational changes. The main monomeric BSA fraction remains stable over 14 days of incubation and demonstrates the stabilizing effect of salt on BSA. In its natural environment (the cells of organisms) the integrity of proteins is also guaranteed by salts along with other cellular components. The salt stabilization effect was proven by the BeNano 180 Zeta Pro.

Under stress conditions (e.g., heat), proteins tend to denature (unfolding, aggregation) which leads to structural changes and the loss of functionality. The BeNano 180 Zeta Pro offers automatic size and zeta potential trend measurements over a predefined temperature range. Fig. 5 demonstrates heat denaturing/sensitivity of BSA. Structural movements of BSA are obvious from decreasing zeta potential values between 30 and 70 °C, whereas particle size remains stable up to 65 °C. From 70 °C BSA denaturation and consequently protein aggregation is reflected by a dramatic increasing Z-ave and rapidly decreasing zeta potential towards 0.

Acoustic attenuation spectroscopy and electroacoustic – DT-1202

For a comprehensive nanoparticle characterization, the acoustic spectrometer DT-1202 provides particle size distribution (acoustic attenuation spectroscopy), zeta potential (electroacoustic) and additional parameters like electric conductivity, pH and temperature. The methods of acoustic attenuation and electroacoustics were already described in detail in Particle World 21 and 22 [9].

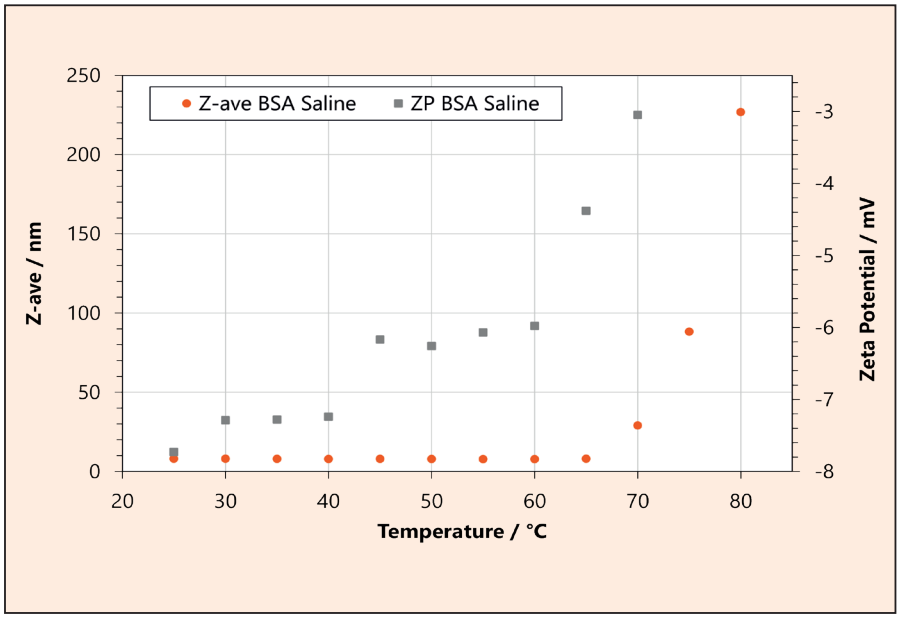

Figure 5 *Heat denaturing of 1 % BSA in Saline (BeNano 180 Zeta Pro)*

Nano-Application of Acoustic attenuation and Electroacoustic

In general, acoustic and electroacoustic can be applied for almost all nanoscale dispersions bigger than 1 nm in D50-value as soon as the concentration of particles in the system is sufficient to produce an appropriate strong attenuation or CVI-signal. For nanoparticles, this is normally not a problem at all because their number is extremely high, even for diluted systems. Nevertheless – especially for size analysis (acoustic attenuation) – soft particles like polymers show too much different specific effects and a clear size analysis is very complex. Thus, the recommendation is to use the DT-1202 for a comprehensive nano-characterization of rigid particles and oil-water-emulsions (water-oil-emulsions cannot be analyzed by electroacoustics).

The aim of the following exemplary study was to manufacture a dispersion of a nanoscale alumina alpha powder with a relatively high solids content and optimal dispersion of the primary particles. To achieve this, the powder was dispersed in a water-isopropanol mixture with a solids content of 20 wt.-%. In a second approach, a steric additive was additionally added before dispersing the powder in the medium using a high-speed dissolver.

The two basis suspensions were adjusted to different pH values using HCl and KOH, as well as zeta potential and electric conductivity were measured. The suspension with the highest zeta potential and the lowest possible electrical conductivity at the same time was chosen to be optimal regarding dispersion conditions and characterized regarding particle size distribution using a DT-1202.The results of the pH-titration experiments are shown in Fig. 6 and 7 as well as Tab. 3.

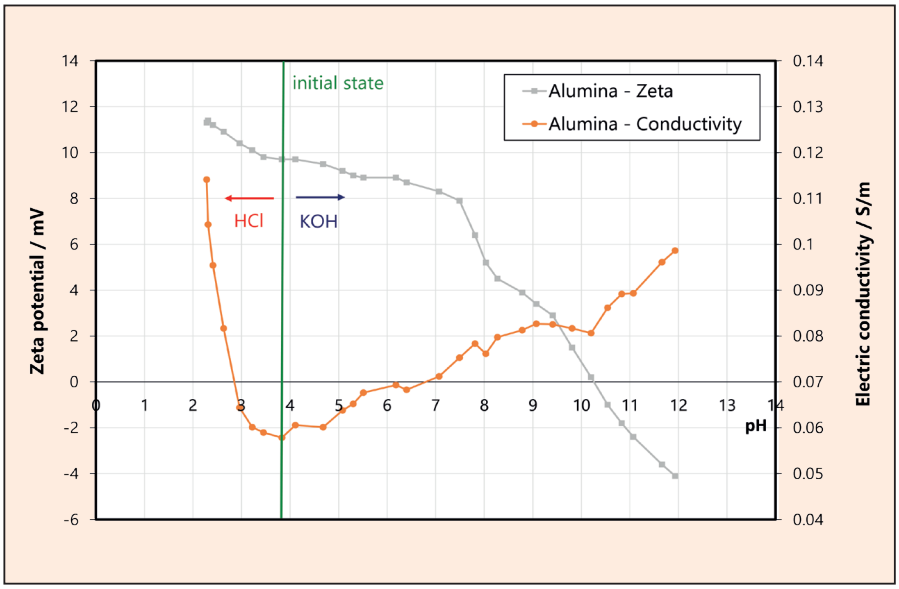

Figure 6 Zeta potential and electric conductivity of alumina vs pH (DT-1202)

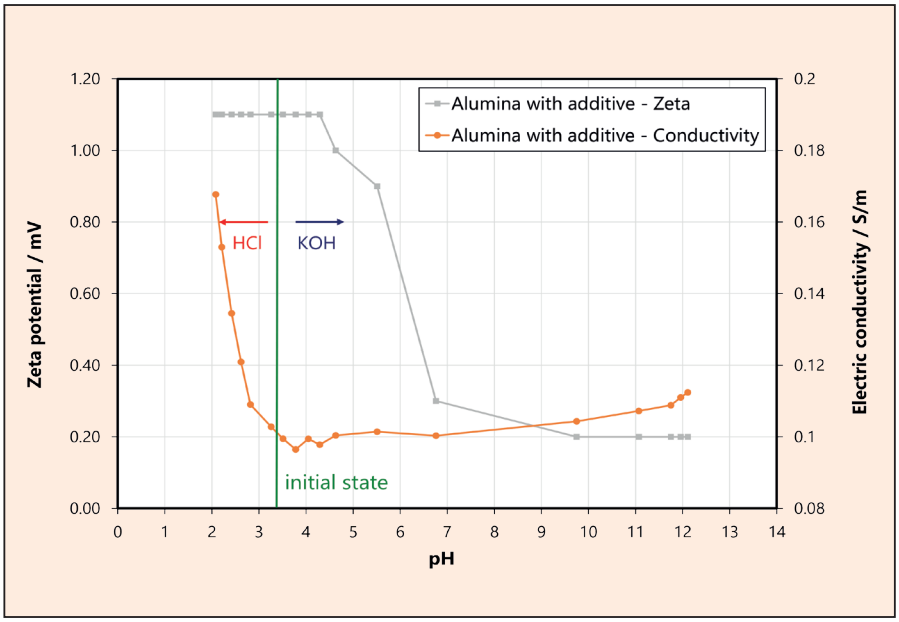

Figure 7 Zeta potential and electric conductivity of alumina with additive vs pH (DT-1202)

Table 3 Results of the titration experiments on alumina

Sample	Dispersed phase	Medium	Solids content / Wt.-%	Start pH	Start zeta / mV	Start el. cond / S/m	IEP / pH	Optimal condition / [mV] / [S/m] / pH
Alumina	Alumina alpha	Water/propanol 60:40	20	3.83	9.70	0.058	10.23	11.40/0.104/2.31
Alumina with additive	Alumina alpha	Water/propanol 60:40 + additive	20	3.78	1.10	0.965	-	1.1/0.965/3.78

Table 4 *Results of the particle size measurements on alumina and alumina with additive*

Sample	pH	Zeta / mV	D10 / µm	D50 / µm	D90 / µm	Size 1 / µm	Size 2/ µm	Vol.-fraction Size 2 / %
Alumina	2.31	11.40	0.042	0.091	0.200	0.091	-	-
Alumina with additive	3.78	1.10	0.029	0.050	0.163	0.049	0.188	18

It can be deducted that the additive has mainly a steric effect, because the zeta potential is very low over the complete pH-range. The optimal dispersing conditions for alumina with additive are the initial ones (pH 3.78, no acid/base). For alumina, the best conditions were found for pH 2.31.

The particle size measurement results for these optimized conditions are given in Fig. 8 (particle size distribution) and Tab. 4.

The measured attenuation spectrum of alumina with additive shows significantly smaller values of the complete range. For rigid solids, the viscous effect is active for very small particles only. This is a proof that the particles are better separated in the system with the additive. This is confirmed by the calculated particle size distribution.

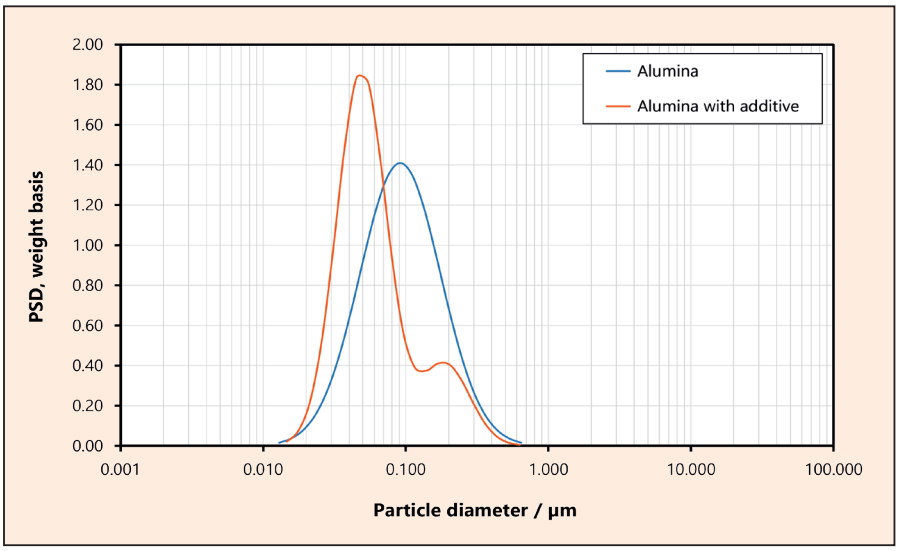

Figure 8 *Particle size distribution of Alumina and Alumina with additive (DT-1202)*

Application guide for optical and acoustic research on colloidal systems

It was shown above that the presented optical and acoustic methods to characterize nanoparticles regarding size and colloidal properties different fields of application. It is up to the user to select the suitable method and use the appropriate experimental setup to get the informative results. Tab. 5 gives an overview to support the correct method selection.

If you have any further questions on the mentioned methods, please contact us at info@3P-instruments.com to discuss your application with us!

Literature

[1] European Commission, Commission Recommendation of 18 October 2011 on the definition of nanomaterial, Off. J. Eur. Union L 275, p. 38–40, 2011.

[2] ISO 22412 Particle Size Analysis – Dynamic light scattering (DLS), 2017

[3] ISO 13099-2 Colloidal systems – Methods for zeta-potential determination – Part 2: Optical methods, 2012

[4] ISO 20998-1 Measurement and characterization of particles by acoustic methods – Part 1: Concepts and procedures in ultrasonic attenuation spectroscopy, 2006

[5] ISO/FDIS 13099-3, Colloidal systems – Methods for Zeta Potential Determination – Part 3: Acoustic methods, 2014

[6] https://www.3P-instruments.com/analyzers/benano_series/

[7] https://www.3P-instruments.com/analyzers/dt-1202/

[8] https://en.wikipedia.org/wiki/Bovine_serum_albumin

[9] Particle World 22 pp. 9 / Particle World 21 pp. 16, available at https://www.3P-instruments.com/particle-world/

[10] Dukhin, A. S.; Goetz, P. J., Characterization of Liquids, Dispersions, Emulsions, and Porous Materials Using Ultrasound, third edition, Elsevier, 3. Edition (8.8.2017); ASIN: B074PN87R5

Table 5 *Scheme to support the method selection for the nanoparticle characterization*

	Nanoparticle characterization – size and zeta potential	
Method	**Acoustic system:** **DT-1202** 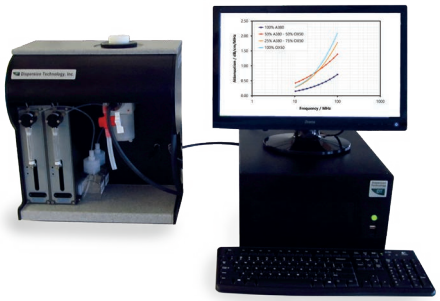	**Optical system:** **BeNano 180 Zeta Plus**
Materials	**rigid particles or oil-water-emulsions** (ceramics, carbon, silica, non-organic pigments etc., opaque oil-water nano emulsion)	**soft particles or emulsions** (polymers, proteins, ingredients, macromolecules, nano colloids, organic pigments etc.)
Typical application	■ characterization and optimization of original dispersions with medium or high solids content, slurry- or paste-like, ■ opaque systems	■ original system with low solids content or diluted samples ■ original systems with high solids content (up to 40 %) ■ translucent systems
Special functions	■ measurements in high conductive or non-polar media	■ measurement of molecular weight ■ trend measurements of size and zeta potential vs temperature ■ temperature control system ■ intelligent intensity adjustment ■ backscattering detection optics: high sensitivity for very diluted samples; applicable for concentrated samples due to an automatic adjustment of the detection point
General sample preconditions (to perform size and zeta potential measurements!)	■ particle size: ≥ 1 nm ■ sample amount: ≥ 3 ml ■ sample concentration: 0.1 – 60 vol.-% ■ temperature range: 7 – 50 °C ■ viscosity: 0.01 – 20000 cp ■ particles are allowed to sediment, stirring and pumping is allowed	■ particle size ≥ 2 nm (DLS only: ≥ 0.3 nm) ■ sample amount: ≥ 0.75 ml (DLS only: ≥ 3 µl) ■ sample concentration: 0.1 – 40 vol.-% ■ temperature range: -10 – 110 °C ■ viscosity: 0.01 – 100 cp ■ particles are not allowed to sediment, neither stirring or pumping is allowed

Comprehensive analysis of soils at the Laboratory for Scientific Particle Analysis (LabSPA)

Dr. Dietmar Klank, dietmar.klank@3P-instruments.com
Dr. Fabian Schönfeld, fabian.schoenfeld@3P-instruments.com

Introduction

Soil is life. The natural functions of the soil, e.g., as part of the nutrient cycle or as a habitat for animals and plants depend on its properties. However, natural soils are among the most difficult materials for particle and surface analysis. This is due to their complex composition as a mixture of different components, all of which exhibit different behavior during sample preparation and analysis. While a microporous fraction of clay needs to be prepared at high temperatures for prolonged periods in order to remove all residual humidity for micropore analysis, these conditions will lead to decomposition or at least a change in the organic humus compounds also present within soils. Optimizing the sample preparation with respect to BET surface analysis is therefore a challenge when it comes to multi-component systems such as soils as opposed to the analysis of pure, single-compound materials, where only the temperature stability of one compound needs to be considered.

In this article, three different soil samples were analyzed by various methods in order to show differences between samples as well as finding plausible interpretations for these variances. The article describes analytical procedures as well as their results and will discuss challenges encountered during the evaluation of complex sample mixtures.

Experimental section

Three different soil samples were taken at different locations throughout Germany: Bavarian forest soil (sample F), Bavarian arable soil (sample A), and North German pasture soil (sample P) (see Fig. 1).

All samples were dried for four weeks at ambient temperature, ground in a mortar and sieved through a 2 mm mesh. Samples of 100 mg each were taken for further investigations. Sampling and preparation of the sieved fractions was carried out by micro-riffling in order to generate representative cross sections for analytical procedures that use small amounts of sample such as particle size analysis or BET surface area. Fig. 1 shows the three samples with their differences, mainly in color. Visual and haptic evaluation of the samples already suggests that sample F could have the highest organic fraction, sample A the highest clay fraction and sample P the highest sand fraction.

Figure 1 *Sample F - Bavarian forest soil (right), sample A - Bavarian arable soil (left), sample P - North German pasture soil (below)*

The residual water content of each sample was determined by measuring the change in mass after drying in a drying cabinet at 105 °C for 24 hours.

The determination of pH-values was carried out as follows: 25 ml of 1-molar KCl solution was added to 10 g of sample in a beaker. The mixture was allowed to settle overnight and pH values were measured with a calibrated pH electrode.

Tab. 1 lists all parameters measured of the samples dried at 105 °C with the corresponding analytical methods at 3P LabSPA. Additionally, thermogravimetric analysis (TGA) and elemental analysis were carried out.

Table 1 *Parameters to be determined, analytical methods and used instruments*

Parameter / Method	Instrument
Bulk density / Standardized powder filling	BeDensi B1
Tap density / Standardized powder tapping	BeDensi T3 Pro
Density / Gas pycnometry	3P densi 100L
Water vapor sorption / Dynamic vapor sorption (DVS)	3P graviSorb 120
Particle size distribution / Laser diffraction Particle shape / Image analysis	Bettersizer S3 Plus
BET surface area / Gas adsorption N_2 at 78 K Gas adsorption Ar at 87 K Gas adsorption CO_2 at 195 K	3P micro 300 3P micro 300 + cryoTune 87 3P micro 300 + cryoTune 195

Results and discussion

Particle size and shape of all three soil samples were determined with a Bettersizer S3 Plus (Bettersize Instruments) by combined application of both laser diffraction and image analysis. Fig. 2 shows the particle size distributions of the untreated samples (dotted lines) compared to sonicated samples treated with ultrasound (solid lines). For sample P (cyan), there is no notable deagglomeration by ultrasound treatment to be observed as both the curve of the raw sample and the sonicated sample are very close to one another. This is different from the samples F (green) and A (red), which show a maximum at 400 µm for the untreated sample (dotted lines). This maximum is still observed after sonication, but deagglomeration caused by ultrasound has led to a notable increase in the fractions of finer particles of < 200 µm.

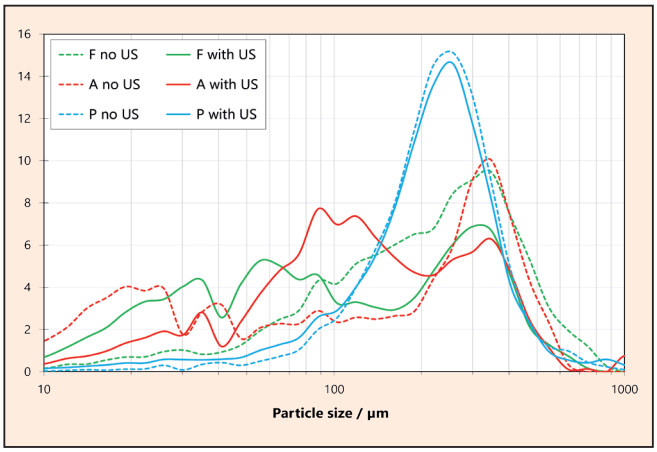

Figure 2 *Particle size distributions of the agglomerated (dotted lines) and deagglomerated (solid lines) soil samples*

An excerpt of the analytical report for sample F is shown in Fig. 3, for which the Bettersizer S3 Plus registered and characterized over 440,000 particles. Fig. 3 shows the particle size distribution determined from shape analysis as well as the distribution of the particles' circularity. It can be seen that most particles have a circularity bigger than 0.8, which indicates shapes close to a sphere. However, a significant fraction of the particles in the coarse range deviates from the spherical shape with circularity values below 0.6.

The thermogravimetric analysis shows significant differences in the ash content of all three samples, which can be seen in the fractions of volatile matter (see Tab. 2). The range up to 105 °C in Fig. 4 indicates that samples F and A bound more water than sample P. Significant differences between samples can be found in the fractions of volatile matter determined by heating up to 925 °C.

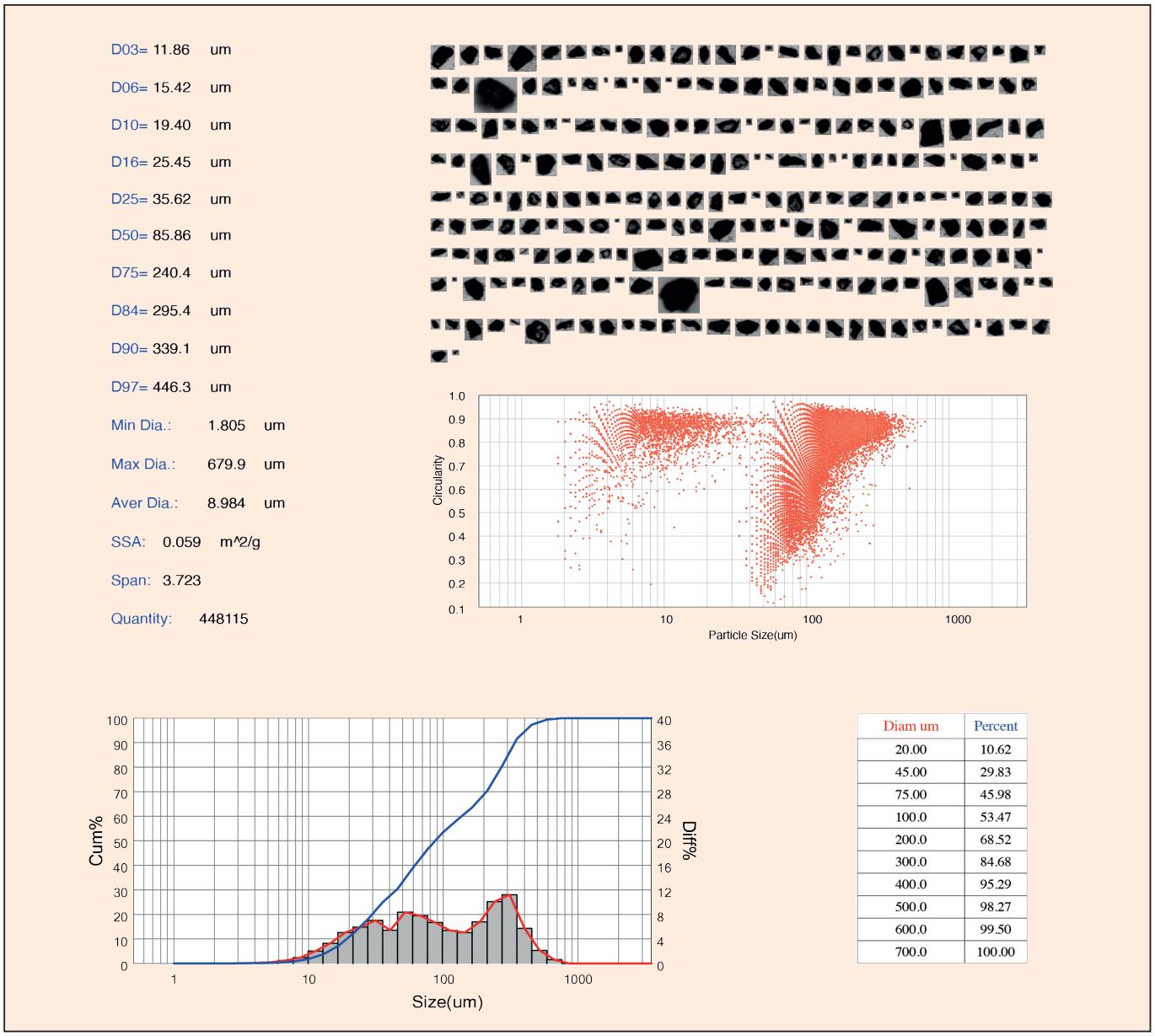

Figure 3 *Part of the report of sample F, particle size and shape analysis of the Bettersizer S3 Plus after ultrasound deagglomeration*

Table 2 *Results of TGA (end temperature: 925 °C) and elemental analyses; moisture content: mass loss up to 105 °C inert; volatile matter: mass loss between 105 °C and 925 °C inert; ash content: residual mass after TG*

Sample	Moisture content / %	Volatile Matter / %	Ash content / %	C / %	H / %	N / %
F	1.19	7.17	91.64	3.57	0.72	0.36
A	1.18	4.14	94.35	1.26	0.46	0.20
P	0.46	1.88	97.58	0.93	0.12	0.11

The water desorption results of the TGA studies below 105 °C are confirmed by the use of the 3P graviSorb 120 to determine the moisture-dependent water adsorption at 20 °C (Fig. 5). Sample P adsorbs significantly less water vapor than the other two samples over the entire range of relative humidity, i.e., the water uptake capacity of F and A is higher than that of P.

The true density of mineral soils is usually found to be between 2.60 g/cm³ and 2.75 g/cm³ as the true density of their main component is Quartz with 2.65g/cm³. As the true density of organic soil compounds is usually between 1.0 and 1.4 g/cm³, the lowest true density value of 2.52 g/cm³ of the samples with sample F and the low pH value (see Tab. 3) can be explained by a high fraction of humic acid in forest soil (see volatile matter from Fig. 4). The tap density corresponds to the organic fraction of the samples – higher organic fractions lead to lower tap density in soil samples.

Particle shape analysis for all three samples resulted in specific surface areas below 0.1 m²/g, which is significantly lower than the BET surface areas measured by physisorption analysis and shown in Fig. 6. This indicates that the specific surface area of the particles is mostly generated from pores. While sand fractions only contribute a negligible amount of surface area, clay and humus fraction are porous materials. Accordingly, the resulting BET surface areas are determined mainly by clay mineral and organic humus fractions. BET surface areas increase for all samples when preparing the samples at temperatures above 220 °C, which indicates to the presence of clay minerals that dispense bound water only at elevated temperatures. Sample preparation below 105 °C mainly increases the BET surface area of sample A, which exhibits the largest surface area of all three samples at these conditions. This indicates that sample F may have the highest fraction of volatile matter, but that the organic fraction of sample F is mainly nonporous. In comparison, sample A has significantly more pores which are filled with residual water at temperatures below 105 °C. A fraction of humic acid decomposes at temperatures between 120 and 220 °C and leads to a decrease of the BET surface area in this temperature range.

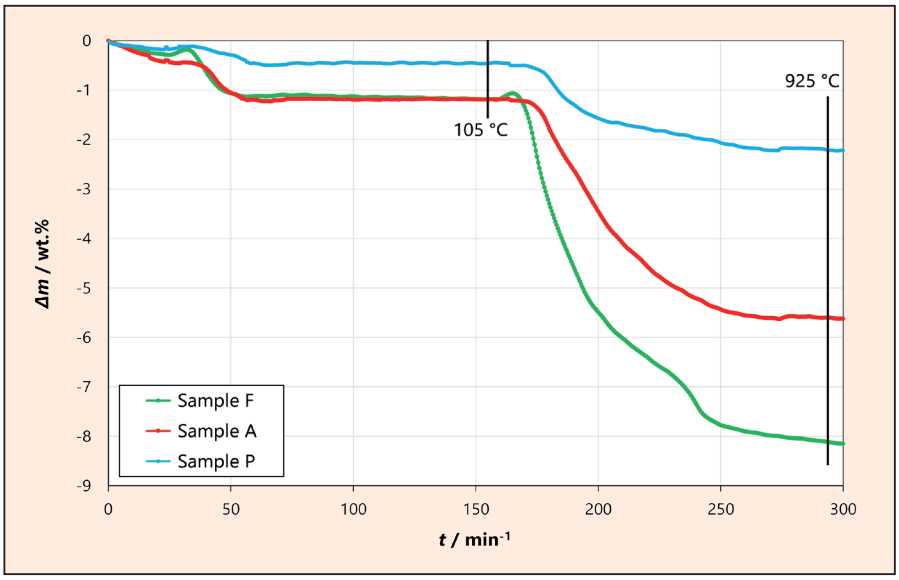

Figure 4 *Thermogravimetric analysis of the soil samples P, A, and F*

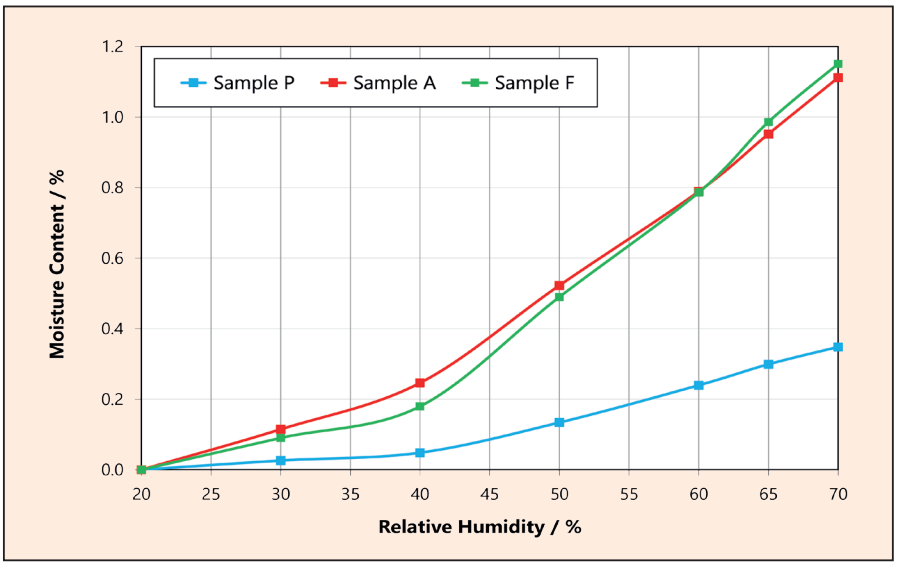

Figure 5 *Results of water vapor sorption at 20 °C measured with the 3P graviSorb 120, showing the different sorption behavior vs. the relative humidity*

Table 3 *pH and density results*

Sample	pH	Bulk density / g/cm-3	TAP density / g/cm-3	Density / g/cm-3
F	3.66	0.90	1.13	2.520
A	6.94	1.14	1.49	2.644
P	6.68	1.44	1.64	2.628

It can be concluded for all three samples that the sample preparation should be carried out at 105 °C in order to achieve comparable results. If the BET surface area of the clay fraction is of interest, samples should be analyzed after preparation at 300 °C additionally. Furthermore, it could be of interest to select different adsorptives for the physisorption analysis.

N_2 at 77 K is the "traditional" standard method for BET surface analysis, but the application of Argon at 87 K has a number of advantages resulting from its noble gas nature as its atoms have a spherical shape in contrast to the ellipsoidal molecule shape of N_2 with unknown positions on the solid surface (effective cross-sectional area of the adsorbate). Because of the unknown adsorbate position of N_2, the Ar-BET values are typically lower to N_2-BET, but more realistic. However, both N_2 at 77 K and Ar at 87 K cannot detect ultramicropores below 0.5 nm because of kinetic restrictions in such small pores and at such low temperatures. The use of an adsorptive at higher temperatures is an alternative to study the existence of such narrow ultramicropores. Hence, CO_2 sorption analysis at 195 K with a cryoTune 195 module from 3P Instruments were conducted, making the variation of analysis temperatures relatively easy. Tab. 4 shows that the differences resulting from CO_2 adsorption are very small in comparison to other adsorptives for samples A and P and can be explained by the difference in cross-sectional area of the gases used. However, sample F shows a different behavior. When measured with CO_2 the BET surface area increases four times in comparison to both N_2 and Ar. This is a strong indicator for the presence of some pores smaller than 0.5 nm. The kinetic restrictions during low temperature gas adsorption measurements of sample F correlates with the highest carbon content of the three soil samples and give an indication that the ultramicropores are part of the humic acid structures. In practice, the nutrient accumulation takes place on the surfaces of the mineral and organic soil particles. The higher the content of smallest pores from clay and humic acids, the more ions can adsorb in these soil micropores.

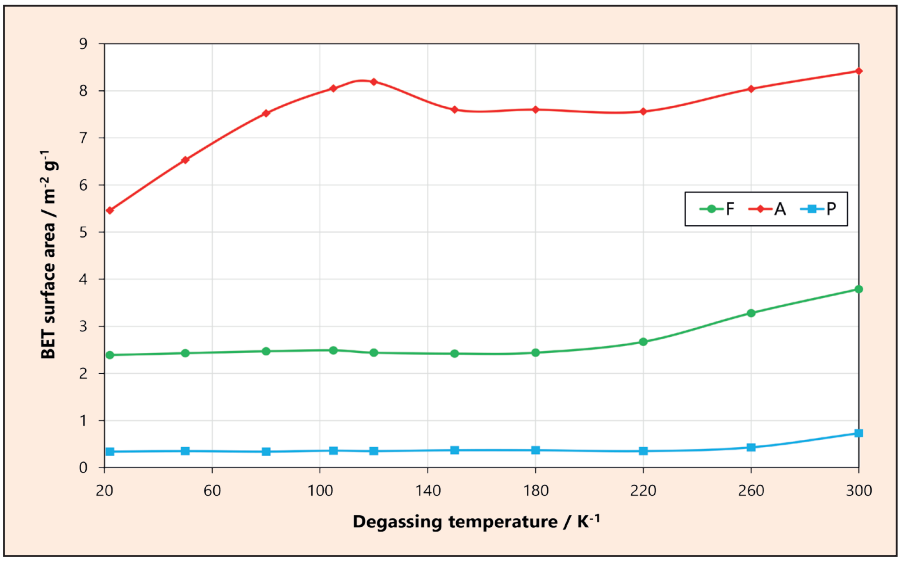

Figure 6 BET surface areas for the three soils dependent on the degassing temperature

Summary

A comprehensive analysis of soil samples with analyzers from 3P Instruments led to statements about particle size and shape, bulk density, tap density and solid density, and about surface and pore structures of the primary particles.

The sample P (North German pasture soil) has the lowest content of volatile matter and carbon, the lowest water rentention capacity, and the smallest BET surface area, but the highest bulk and tap densities because it has the highest sand content.

Sample A (Bavarian arable soil) has a higher content of volatile matter as compared to sample P and consequently a lower ash content. The comparison of the densities (bulk, tap and true densities) gives the indication that most of the micropores occur in mineral structures like clay. These pores seem to be larger than 0.5 nm, which can be deducted from the similar BET surface areas calculated from adsorption measurements with N_2, Ar and CO_2.

Sample F (Bavarian forest soil) with the highest organic content has the lowest densities (bulk, tap and true densities). The differences in the BET surface area of CO_2 to N_2 and Ar gives strong indication of ultramicropores in the humic acid structure of that soil sample.It needs to be considered that for a sensible comparison of BET surface areas of soil samples a useful degassing temperature needs to be selected for all samples. To study the micropores (< 2 nm) and ultramicropores (< 0.5 nm) of soils, such samples should also be analyzed with complementary detailed gas adsorption analysis carried out with CO_2 at 195 K.

The LabSPA (Lab for Scientific Particle Analysis) provides a variety of different analytical procedures for a broad spectrum of solid materials. We are happy to help you with our experience and you can contact us at info@3P-instruments.com or inform yourselves at www.3P-instruments.com, where we highlight new developments.

We gratefully acknowledge the contribution of Apostolos Ergenekon made during his practical term at 3P Instruments for running the analysis used herein and we thank the Institut für Nichtklassische Chemie e. V. in Leipzig for carrying out elemental analysis and TGA.

Table 4 BET surface area determined with different adsorptives (samples degassed at 105 °C)

BET / m^{-2} g^{-1}	N_2 77 K	Ar 87 K	CO_2 195 K
Sample F	2.47	1.62	11.06
Sample A	8.05	7.90	10.26
Sample P	0.36	0.34	0.82

Invitation to the Adsorption event series and review of our Adsorption Week 2022

Dr. Denise Schneider, denise.schneider@3P-instruments.com

Free webinars on Gas Adsorption - "Sorption World"

We have decided to launch a webinar series "Sorption World" in September 2022 to complement our biannual scientific 3P events. The webinars are aimed at anyone interested in sorption worldwide, regardless of the analytical instrumentation they are working with. Here is an overview of the upcoming events:

- **13th September 2022** — **What all can go wrong? Gas adsorption measurements in the lab**
  An outline of challenges, possible errors and their solutions in measurements of static adsorption isotherms in all forms.
- **22nd November 2022** — **Online Symposium**
  One-day meeting of international scientist who share their recent results - abstract submission open.
- **24th January 2023** — **Do adsorptive parameters really play a role?**
  A detailed story about the use of adsorptive parameters and the impact on both your measurement and data evaluation.
- **21st March 2023** — **How can different adsorptives be used to effectively characterize micropores?**
  Sometimes a combined approach of different adsorptives is necessary to get reliable results. We will show possibilities, limits and challenges.

If you have specific questions about the respective webinar, please do not hesitate and send us your questions in advance to info@3P-instruments.com, so we will try to answer them in the webinar discussion, or in direct email contact.

Registration is now open at www.3P-instruments.com/events

Invitation to Adsorption Week 2023

Our next hybrid annual meeting on adsorption & characterization of porous materials will take place on 25th - 27th April 2023. Registrations for online participation or on site possible at www.3P-instruments.com/events

Not sure what to expect?
Read the review of 2022 (see next page).

Review of the Adsorption Week 2022

Over 150 international participants took part in the two-day conference on gas adsorption and related techniques for the characterization of porous materials, hosted by 3P Instruments and the Institut für Nichtklassische Chemie e.V. (INC).

As the conference was a hybrid event, the lecture program with 15 national and international speakers from academia and industry included talks streamed from overseas and live at the venue in Leipzig. We were glad to welcome and hear the talks of Prof. em. Rouquerol and Prof. Kaskel on the topics „Special interest of sample-controlled heating for the thermal treatment of adsorbents" and "Adaptive metal-organic frameworks" on site. Via Livestream, e.g. Dr. Daniel Siderius (USA) and Prof. Diana Azevedo (Brazil) gave their lectures from thousand kilometers away from Germany. Nevertheless, after each lecture, the auditorium questioned the speaker and fruitful discussions of aspects of their talk started. The conference was completed by talks of industry representatives such as Christina Schneidermann from HERAEUS and Johan Craeye from Desotec.

During the numerous breaks, the participants got in touch with each other, discussed talks and questions, connected and started cooperations. Experts from INC and 3P Instruments were consulted on theoretical and practical issues about static and dynamic adsorption and gave hands-on experience with the analysis instruments mixSorb L for breakthrough analysis, and the cryoTune option for accurate and flexible temperature control during gas adsorption measurements.

In addition to the two-day conference, we offered PhD students an additional one-day workshop on "poster presentation" with an interactive character. The attendees got scientific and structural input from Dr. Sebastian Ehrling and Dr. Denise Schneider (both 3P Instruments) as well as from Dr. Jens Möllmer (Institut für Nichtklassische Chemie e.V.) and trained their scientific poster presentations by presenting other people's posters in a poster karaoke session.

SACHSEN

This event was co-financed with tax funds on the basis of the budget passed by the Saxon state parliament.

Figure 1 *Dr. Sebastian Ehrling demonstrating the cryoTune option*

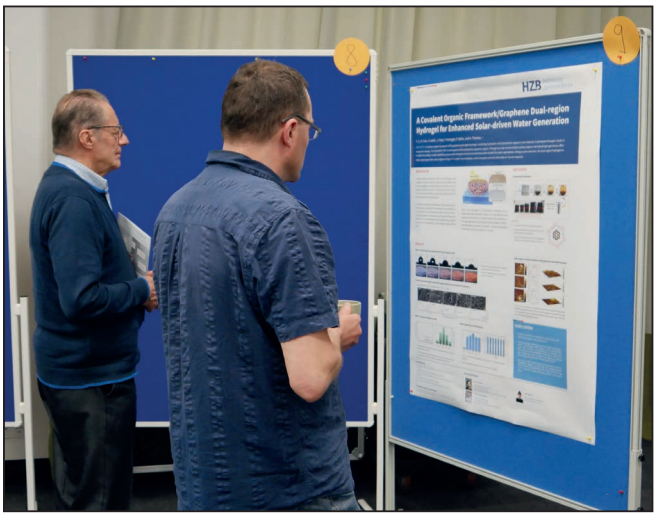

Figure 3 *Prof. em. Jean Rouquerol reading a poster exhibited by a PhD student*

Figure 2 *Prof. Diana Azevedo giving a remote talk from Brazil*

Figure 4 *Poster karaoke session of the PhD students*

Investigation of Industrial Adsorbents for Carbon Capture by Gas Flow Methods

Dr. Sebastian Ehrling, sebastian.ehrling@3P-instruments.com
Francesco Walenszus, francesco.walenszus@3P-instruments.com

mixSorb L

3P meso 400

Introduction

After a long period of remote-only conferences and meetings, the "Fundamentals of Adsorption" took place in Denver a couple of months ago. Traditionally, this is one of the major events for the adsorption-community and a lot of attendees from or all over the world are participating in person. However, one significant goal of this conference is to take part in the reduction of its participants CO_2 footprint. Therefore, for the first time, the conference was carried out as hybrid event, meaning that almost all contribution as presentations and poster were additionally presented online.

Moreover, from ten technical sessions as much as six dealt with carbon capture/separation and environmental questions, showing the tremendous necessity to work on solutions regarding this and protect our ecosystem. Primarily the following three major fields were discussed:

1. Direct air capture:
   400 ppm CO_2 in N_2 under dry and wet conditions
2. Flue gas purification:
   15 % CO_2 in N_2 under dry and wet conditions
3. Bio gas purification:
   ~5 % CO_2 in CH_4 under dry and wet conditions

Currently, many different approaches are proposed to capture carbon from the environment. Adsorption techniques offer the opportunity to separate gases with low energy consumption. In the literature, numerous materials are discussed and proposed for this challenge. All materials, independent of their nature, however, have in common that they need to be precisely characterized before use. The common workflow is presented in Fig. 1 (see next page). Within 3P Instruments, our expertise covers the first three steps, despite the synthesis of the materials.

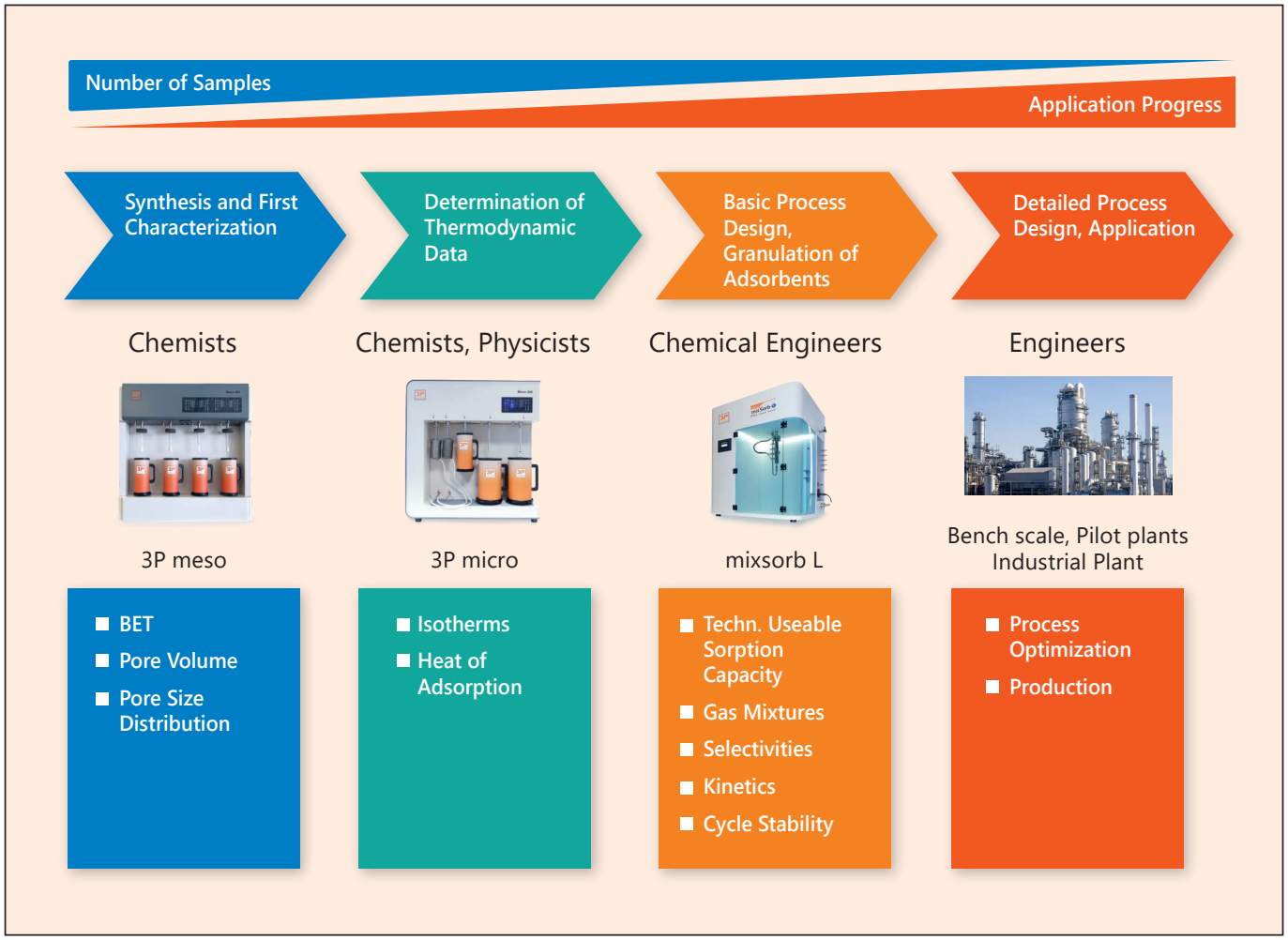

Figure 1 *Workflow: From material development to final application*

Assuming one has a very interesting material on hand, we will discuss the general workflow that 3P Instruments can offer. In general, a low-pressure isotherm at a certain temperature is collected to determine the capacity of the material. With that, access to characteristic values, such as surface area, pore volume or pore size distribution can be also gained. In addition, it is feasible to measure at different temperatures to determine the isosteric heat of adsorption, which gives a first glimpse about the possible behavior of the material under dynamic conditions. With that value, not only the adsorption but also the desorption might be predicted [1]. A major challenge for every promising material lies in the uptake of CO_2 in the presence of water [2-4]. However, with static methods one could measure as well a water vapor isotherm at the respective temperature and possibly might predict the adsorption behavior of the material under humid conditions by applying the IAS theory. A more elegant and reliable method, however, is the use of dynamic methods which allows the simultaneous dosing of gases and vapors.

In the following article, we are aiming to describe a possible material characterization pathway. The obtained results can be useful for both academia and industry, since material screening is possible as well as quality control for existing processes.

Experimental

Material

For all investigations, an activated carbon D55/1.5 from Blücher GmbH was used. The particle size dimension is around 3 mm. For better sample handling during the static measurements and dynamic measurements in a small adsorber (inner diameter (ID) 6 mm), the sample was ground to obtain a powder. Prior each measurement the sample was pre-treated at 150 °C either in dynamic vacuum (static measurement) or inert gas flow (dynamic measurement) over night.

Instrumentation

Static CO_2 isotherms were collected on a 3P micro 200 [5]. The temperature was set with a cryoTune 195 [6] to precisely control the adsorption temperature. Dynamic breakthrough experiments were performed on a mixSorb S [7] and mixSorb L [8] with 6 mm (ID) and 3 cm (ID) adsorber respectively. Both instruments are equipped with an evaporator to allow the simultaneous dosing of gases and vapors. For binary mixtures, the included thermal conductivity detector (TCD) can be used. However, for more complex mixtures a mass spectrometer from MKS was attached.

Software

Data evaluation and simulation was performed with mixSorb manager and 3P sim.

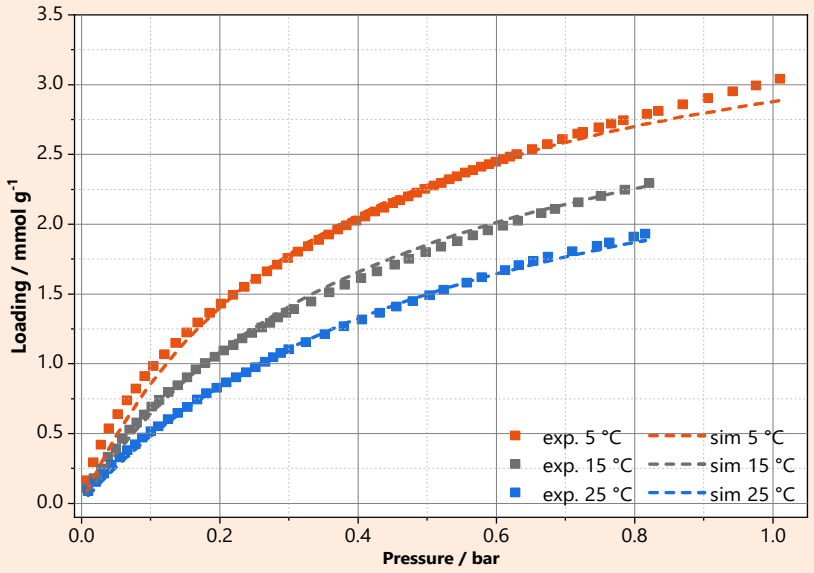

Temperature	**5 °C**
Affinity Constant	2.803843 bar^{-1}
Maximal Loading	3.905042 mmol g^{-1}
Determination Coefficient R^2	0.992677
Temperature	**15 °C**
Affinity Constant	2.220004 bar^{-1}
Maximal Loading	3.522760 mmol g^{-1}
Determination Coefficient R^2	0.996550
Temperature	**25 °C**
Affinity Constant	1.785483 bar^{-1}
Maximal Loading	3.177901 mmol g^{-1}
Determination Coefficient R^2	0.998039
Heat of adsorption	**15.5 kJ mol^{-1}**

Figure 2 *Fitting results using Langmuir model*

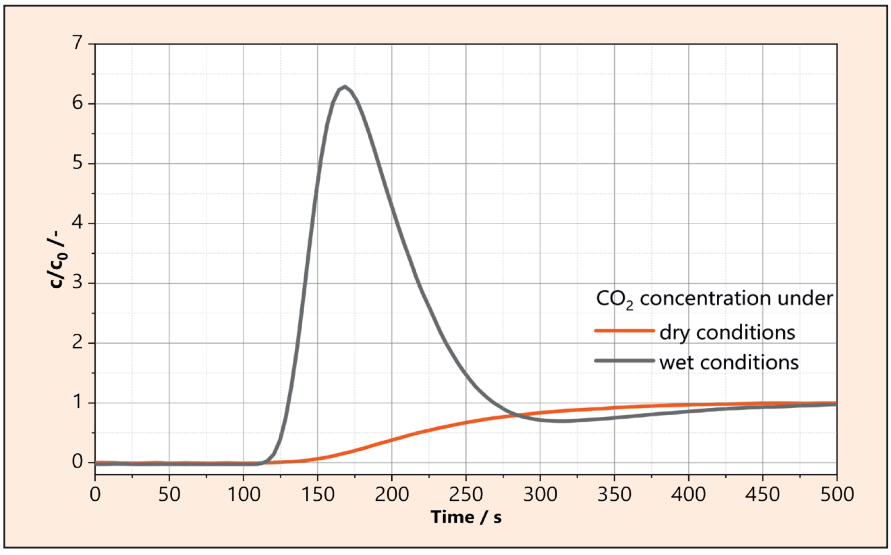

Figure 3 *Breakthrough curve of 400 ppm CO_2 in N_2. Total flow: 125 mL min^{-1}, p = 1 bar and T = 25 °C. Wet conditions: 80 % Humidity, Evaporator temperature: 33 °C.*

Results

Static measurements

Static CO_2 isotherms were collected at three different temperatures, namely 5 °C, 15 °C and 25 °C and fitted using the Langmuir model, which is included in the 3P sim Software package. The results of the adsorption and fitting are shown in Fig. 2.

As expected, CO_2 shows a higher affinity at 5 °C with respect to the elevated temperatures. This results in a steeper uptake at low pressure and an overall higher maximal loading. These parameters can be used to get an idea about the later performance of a material, such as the behavior during a temperature swing adsorption.

Dynamic breakthrough experiments

As mentioned in the beginning, CO_2 capturing or separation, respectively, is mainly discussed in the course of direct air capture, flue gas purification and bio gas separation. The mixSorb series allows the simultaneous dosing of two or more gases and/or vapours. Therefore, 3 different experiments were designed with varying CO_2 concentrations, under dry and humid conditions and with CH_4 in N_2 at ambient pressure and 25 °C. The flow rates were adapted to the MFCs present in the devices and due to that could not be kept constant over all experiments.

Measurements using mixSorbS

The mixSorb S device is designed to allow measurements with low sample amounts from 1 to 8 bar. In this study, an adsorber with 6 mm inner diameter and a packing height of 6 cm was used which enables a loading of around 1 g of activated carbon powder. The vapor is generated by a heated bubbling system. Typically, the carrier gas is bubbled through a liquid and by adjusting the flow rate of the carrier gas, the evaporator temperature, and the adsorber temperature, relative humidities between 0 and 85 % can be generated. In the following experiments a relative humidity of 80 % was generated by bubbling N_2 through water, further noted as "wet conditions".

All following data evaluation is done purely qualitative, since the aim of this study is not to study the material, but rather show the feasibility of the mixSorb devices and a possible material characterization workflow.

In a first experiment, a direct air capture experiment is done, by dosing 400 ppm CO_2 in nitrogen. At 100 kPa (1 bar) this equals a partial pressure of CO_2 in the column of 0.04 kPa. Since the total flow of the mixSorb S devices is limited by the used MFCs, a pre-mixed gas was used. By diluting 1 mL of a 5 % CO_2 in N_2 with 124 mL of pure nitrogen the desired mixture can be generated at a moderate total flow rate. The results are shown in Fig. 3 (orange curve). A rather long breakthrough is observed with slow kinetics. Under real conditions, however, water is always present which is why it is of utmost importance to study CO_2 adsorption also under wet conditions. The grey curve in Fig. 3 shows the simultaneous adsorption of CO_2 and water. In contrast to the previous experiment, an almost spontaneous breakthrough of CO_2 is observed, showing the higher affinity towards H_2O with respect to CO_2. In the beginning of the experiment a steep increase of the CO_2 is observed which is followed by a pronounced roll-up of CO_2 - the immediate desorption of CO_2 due to the water adsorption in the fixed bed.

Many people are looking into the separation of CO_2 from flue gas. Usually, one can find around 15 % CO_2 in such a gas stream. Thanks to the great flexibility of the mixSorb devices (e.g., up to 4 different MFCs), studies under these conditions are possible. Compared to the previous experiment, a significant steeper breakthrough is observed, since the partial CO_2 concentration is 375 times higher (0.04 kPa vs 15 kPa) under these conditions. Unfortunately, one cannot directly compare the breakthrough times, since the total flow rates are different. Once again, the experiment was done under dry and wet conditions, since normally a flue gas stream also contains water.

In the last experiment, a slightly more complicated matrix was tested - the separation of CH_4 and CO_2 from a "natural gas stream" under dry and wet conditions. Obviously, the composition of natural gases depends on its origin and deviates

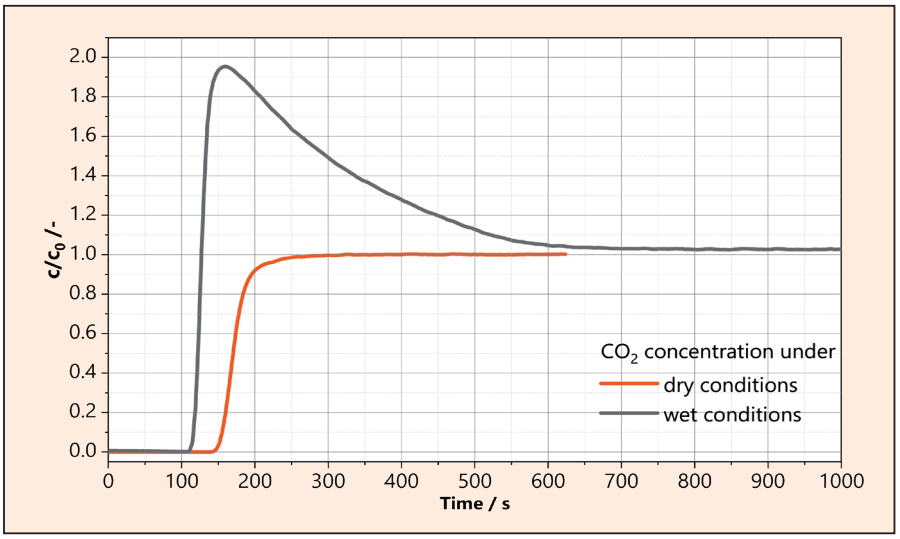

Figure 4 *Breakthrough curve of 15 % CO_2 in N_2. Total flow: 45 mL min^{-1}, p = 1 bar and T = 25 °C. Wet conditions: Evaporator temperature: 33 °C.*

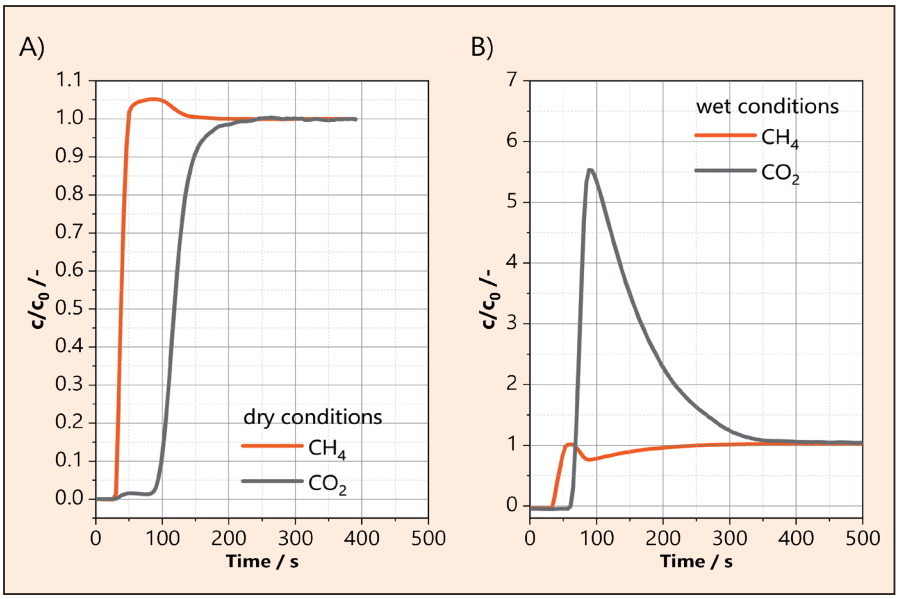

Figure 5 *Breakthrough curve of*
A) *85 % CH_4, 5 % CO_2 in N2. Total flow: 70 mL min-1, p = 1 bar and T = 25 °C.*
B) *82.5 % CH_4, 5 % CO_2 2.5 % H_2O in N_2. Total flow: 70 mL min-1, p = 1 bar and T = 25 conditions: Evaporator temperature: 24 °C.*

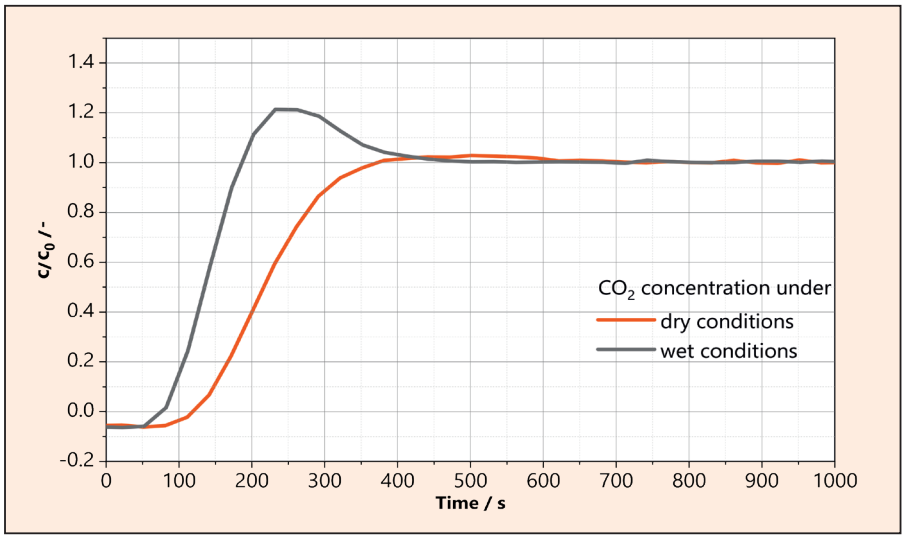

Figure 6 *Breakthrough curve of 400 ppm CO_2 in N_2. Total flow: 8541 mL min^{-1}, p = 1 bar and T = 25 °C.*

from source to source. However, typically one can find between 85 – 96 % CH_4, around 5 % CO_2 and nitrogen in the stream.[9]

We therefore designed an experiment with 85 % CH_4, 5 % CO_2 and 10 % N_2 under dry and wet conditions.

Methane does not show any adsorptive interaction with the sample, which results in a spontaneous breakthrough. The CO_2 curves under dry and wet conditions are comparable to the previous experiments.

Measurement using mixSorb L

After a successful screening on the mixSorb S with low sample amount, we proceeded with the mixSorb L. This device was designed to use a higher sample loading and since the dimensions of the adsorber are bigger than the mixSorb S adsorber it is also possible to investigate already processed materials like extrudates or beads. With the mixSorb L pilot plants can be mimicked to some extend on the lab scale. To be as close as possible we decided to use for all following experiments a superficial velocity of 0.2 ms^{-1} which equals a flow rate of 8.5 L min^{-1} (STP) in a 3 cm (inner diameter) adsorber. The remaining parameters, such as temperature, pressure and analyte concentration were kept constant regarding the previous performed experiments on the mixSorb S. One additional difference between the mixSorb S and the mixSorb L device is the way of vapor generation. As already mentioned, the mixSorb S device uses a bubbling system. In the mixSorb L an independent evaporator utilising a Coriolis type mass flow controller for precises liquid dosing to a hot surface is used.

Fig. 6 shows the comparison of the dry and wet breakthrough of pelletised material measured in the mixSorb L. As expected from prior experiments the dry breakthrough takes more time and therefore reaches higher capacity than the wet breakthrough. The roll-up effect in the wet experiment is also visible but not as pronounced as for the experiments in the mixSorb S device. In addition, it can be clearly seen from the slope of the breakthrough that with the pelletised material the kinetics of CO_2 breakthrough are improved.

The other two mixtures namely flue gas and biogas are still under investigation with the mixSorb L device and are therefore omitted here for the moment.

Conclusion

Within this study, we were aiming to show a possible workflow for the proper characterization of your promising adsorbent materials. From an initial static-volumetric experiment, it is possible to get a first insight into the adsorption properties of your material and the isosterical heat of adsorption can be calculated. Furthermore, it is also possible to simulate a dynamic measurement with the 3P sim software package. Even this was not within the scope of this investigation, it also helps to get a well-defined starting point for your dynamic experiments.

For the dynamic experiments, the mixSorb series offers tremendous possibilities to realise different dynamic breakthrough experiments. With the mixSorb S, it is possible to get mainly equilibrium data for small sample amounts. Due to the small columns coming with the device and the minimal flow rates, the investigation of materials in research state and powders has never been easier. Thinking one step further towards industrial application, the mixSorb L can be used to study already processed materials and additionally obtain more reliable kinetic data as well as information about temperature profiles along the column.

3P Instruments offers a full set of devices to characterize your adsorbent materials on its way to the application and get reliable measurement data before setting up a test plant. If you have any further questions, please contact us at info@3P-instruments.com – we are happy to help!

Literature

[1] S. Builes, S.I. Sandler and R. Xiong Isosteric heats of gas and liquid adsorption. Langmuir, 29 (2013), 10416-10422.

[2] N. Chanut, S. Bourrelly, B. Kuchta, C. Serre, J.-S. Chang, P.A. Wright, P. L. Llewellyn, Screening the effect of water vapour on gas adsorption performance: application to CO_2 capture from flue gas in metal–organic frameworks, ChemSusChem. 10 (2017) 1543–1553.

[3] G. Li, P. Xiao, P. Webley, J. Zhang, R. Singh, M. Marshall, Capture of CO_2 from high humidity flue gas by vacuum swing adsorption with zeolite 13X, Adsorption 14 (2008) 415–422.

[4] A.S. Palakkal, R.S. Pillai, MFFIVE-Ni-L (M=Fe/Al, L=pyr), with Coordinatively Unsaturated Metal Site for CO2 Separation from Flue Gas Composition in Presence of Humidity by Computational Methods, Dalton Trans. 50 (2021) 466–471.

[5] https://www.3P-instruments.com/analyzers/3p-micro/

[6] https://www.3P-instruments.com/analyzers/cryotune/

[7] https://www.3P-instruments.com/analyzers/mixsorb-s/

[8] https://www.3P-instruments.com/analyzers/mixsorb-l/

[9] S. Faramawy, T. Zaki, A.E. Sakr, Natural gas origin, composition, and processing: A review. Journal of Natural Gas Science and Engineering, 34 (2016) 34-54.

New partnership for capillary flow porometers – 3P Instruments and Poretech

Dr. Fabian Schönfeld, fabian.schoenfeld@3P-instruments.com
Dr. Carsten Blum, carsten.blum@3P-instruments.com

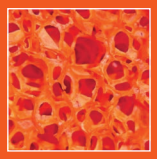

The characterization of through pores is gaining more and more importance with the emergence of new battery technologies as well as the increasing needs for durable papers required for the manufacturing of cardboard, to name only two examples. Both membranes and paper require a method to consistently and reproducibly measure the through-porous structures they contain, as these characteristics define their functionality. 3P Instruments would therefore like to announce a new partnership regarding the development and support of capillary flow porometers. Our new partner is Poretech Instrument Inc. and can rely on decades of experience regarding the manufacture of porometry equipment.

The new line of INNOVA porometers will incorporate a number of features that will increase the overall quality of datasets acquired with capillary flow liquid extrusion techniques as well as gas flow and liquid flow characterization to determine resistivity of porous materials. The INNOVA series consists of three different models, which can be customized towards the applications required in any clients laboratory whilst retaining ease of use over all methods available.

INNOVA iCFP models

The INNOVA iCFP models are the basic version for performing gas and liquid permeametry analysis as well as capillary flow porometry. Permeametry is based solely on the gas flow through a given sample and will yield air flow resistivity values as well as qualitative indicators towards the materials behavior under increased pressure. Capillary flow porometry is a liquid extrusion method to determine a pore size distribution for a given through-pore system by means of applying pressure on one side of a pore and extrude a wetting liquid that has filled all accessible pores prior to analysis. The analysis will usually yield three cardinal points such as bubble point (largest pore), MFP (Mean Flow Poresize) and smallest pore (see Fig. 1).

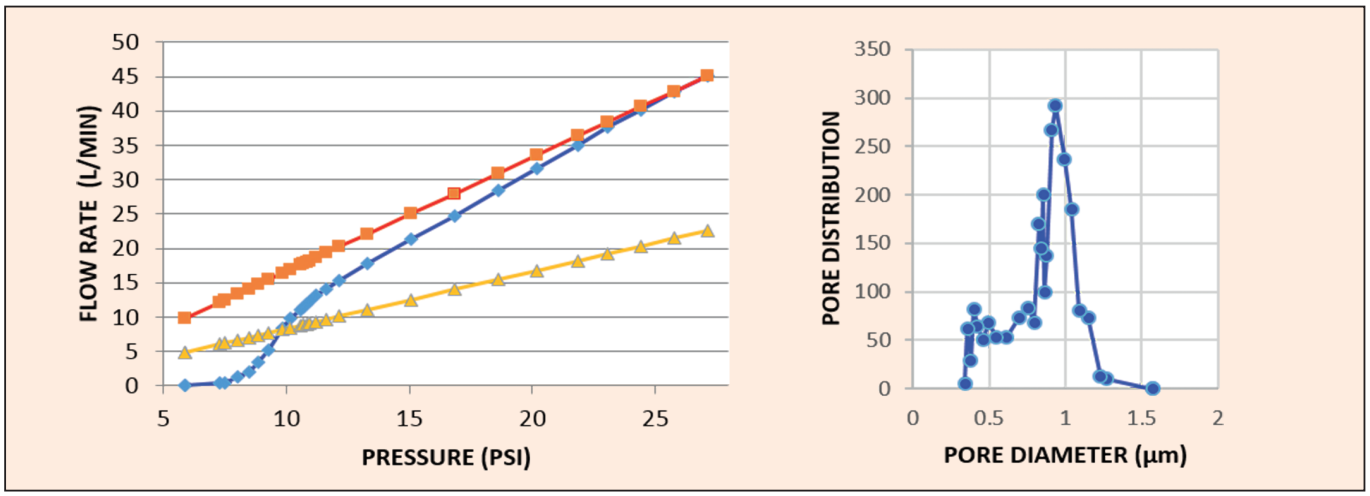

Figure 1 *Standard CFP measurement with bubble point (largest pore), MFP (Mean Flow Poresize) and smallest pore*

The INNOVA-series porometers are equipped with a bubble-point detection setup that relies on a pressure regulator instead of a flow meter which dramatically enhances sensitivity towards the first gas flow through a sample thus increasing the precision with which the largest pore of a material will be determined. After bubble-point detection, the instrument will switch towards a flow-meter assembly to determine cumulative filter flow and calculate pore size distributions. Basic instruments can determine a pore size range from 80 µm down to a minimum of 60 nm and can be upgraded to a maximum range from 500 µm down to 13 nm.

INNOVA iLLP models

The INNOVA iLLP models are instruments tailored towards a special type of capillary flow porometry that is called "liquid-liquid-porometry". It relies on decreasing the surface tension of a wetting liquid inside a given through pore system by immersing the sample in a second liquid rather than having an interface between the wetting liquid and a pressurized gas. As a result, the surface tension of the standard wetting liquid Galpore (which is a perfluorated carbohydrate) of 15.9 dyn/cm can be decreased to 4.5 dyn/cm when brought into contact with isopropyl alcohol. This shifts the accessible pore range from the aforementioned 500 µm to 13 nm to significantly smaller values of 300 nm down to a minimum of 2 nm for a fully upgraded INNOVA iLLP porometer.

INNOVA iUNP models

The INNOVA iUNP models represent the combination of both the iCFP- and the iLLP-models and offer customers the highest flexibility when it comes to analyzing through pore materials. The iUNP-models are equipped with two sample chambers, one suitable for the standard gas-liquid capillary flow porometry and the other one suitable for the liquid-liquid porometry setup. A fully upgraded iUNP-model provides an analytical range from 500 µm down to a minimum of 2 nm.

Additional features

The INNOVA-series of porometers can be equipped with a number of different features and 3P Instruments can provide custom solutions for more challenging solutions. Among the standard features are special sample holders for hollow fiber membranes and rapid clamp-on holders for irregularly shaped flat sheets. Wetting liquids as well as spare parts and tailored sample holders can be acquired from 3P Instruments. Please do not hesitate to contact us with your questions under info@3P-instruments.com or +49-(0)-8134-9324-0.

Table 1 *INNOVA series models and pore ranges*

Models	Max. 100 psi	Max. 200 psi	Max. 500 psi
iCFP	80 µm – 60 nm	80 µm – 30 nm	80 µm – 13 nm
iLLP	–	300 nm – 6 nm	300 nm – 2 nm
iUNP	–	80 µm – 6 nm	80 µm – 2 nm
Extended Range option	max. 500 µm	max. 500 µm	max. 500 µm

Service for instruments from Cilas, Quantachrome, Altamira and our current product range

service@3P-instruments.com

As the former Quantachrome GmbH, we as 3P Instruments continue to look after the analytical instruments from the manufacturers Cilas, Quantachrome, and Altamira.

Service and spare parts

Our more than 30-years experienced service department will continue to service the following analytical instruments:

- Cilas 920, 930, 990, 1064, 1180, 1090, 1190
- Quantachrome devices, e.g., Autosorb, or NOVA, and many more.

Before assuming that your older Cilas or Quantachrome device is beyond repair, be sure to contact service@3P-instruments.com for a free consultation.

3P Instruments still offers service and maintenance contracts, as well as spare parts, accessories and consumables, please see the examples:

- for Cilas particle sizers: measuring cell (cuvette), tubes, stirrer parts, motors for stirrer etc.
- for Quantachrome analyzers: measuring cells of all possible types for physisorption and chemisorption, filler rods, fill funnels, filers, heating mantles, Dewars, standard materials, and others.

Don't hesitate to send request for the spare parts catalog, simply send an email to info@3P-instruments.com with the type of your analyzer.

Second hand instruments as economic and ecological alternative

In addition to the service, maintenance and spare parts, the purchase of Cilas and Quantachrome used equipment through our customer-friendly 3P service can still be worthwhile. Our service offers and used equipment are both economically and ecologically reasonable: Check with 3P Instruments whether the further operation of your laser granulometer or gas sorption device is advisable! Save resources and save yourself a possibly unnecessary change of equipment in the laboratory.

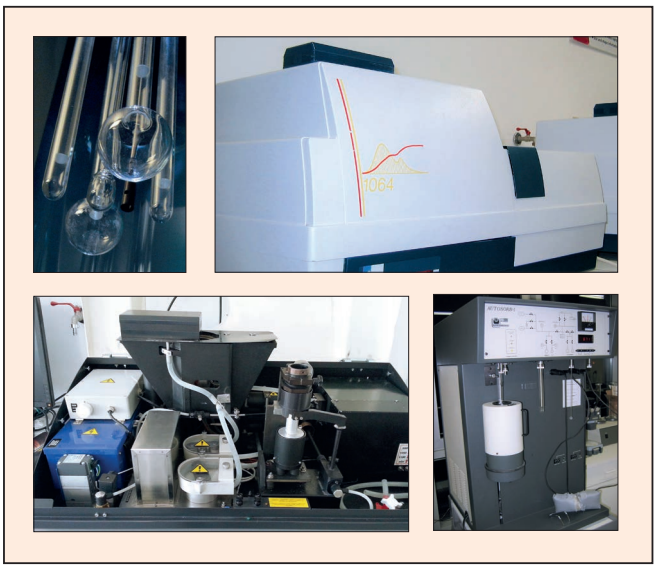

Figure 1 *Examples of 2nd hand devices: we have the instrument, but also the spare parts and consumables available*

Table 1 *Examples of available second hand instruments*

Second hand instruments	Producer	Description	Price / Euro
Poremaster 33	Quantachrome	mercury porosimeter	18,000
Poremaster 60	Quantachrome	mercury porosimeter	20,000
Autosorb-1MP	Quantachrome	BET surface, micro- and mesopore analysis	12,000
Autosorb-1MP	Quantachrome	BET surface, micro- and mesopore analysis	15,000
Autosorb-3B	Quantachrome	BET surface, mesopore analysis, three measuring ports	9,000
Autosorb-1-C-vapor	Quantachrome	BET surface, micro- and mesopore analysis, chemisorption, and vapor sorption	20,000
Pentapyc	Quantachrome	density of solids, five measuring ports	4,500
CILAS 930L	Cilas	laser particle sizer 0.2 - 500 µm	12,000
CILAS 920L	Cilas	laser particle sizer 0.3 - 500 µm	12,000
CILAS 920L	Cilas	laser particle sizer 0.3 - 500 µm	10,000
CILAS 920L	Cilas	laser particle sizer 0.3 - 500 µm	10,000
CILAS 1064L	Cilas	laser particle sizer 0.3 - 500 µm	15,000
Cilas 1180L	Cilas	laser particle sizer 0.04 - 2,500 µm	15,000
Occhio FS 200	Occhio	particle size and shape 0.4 - 1,000 µm	10,000
Nanoptic 90	Bettersize	particle sizer DLS	14,900

New head of 3P service department

We would like to thank Gerd Scharschuh for his more than 30 years of commitment, initially at Quantachrome GmbH and in recent years at 3P Instruments. Gerd is the best Cilas specialist we know worldwide! But many of our customers and international partners also know Gerd as the Quantachrome specialist who was involved in endless ideas, further developments and software tests.

And we are very happy that Gerd will be available to advise us for a while after he has handed over his responsibilities as service manager, so that we don't immediately miss all his creative and fast problem solving.

In a small farewell party with the entire company, Gerd Scharschuh was presented with some gifts and given a fitting farewell as service manager.

Peter Macht, a colleague of many years, has taken over the management of the department as of August 1st, 2022.

Are you interested in second hand devices, spare parts for Cilas or Quantachrome instruments, or simply want to send a message to Gerd or Peter?

Get in touch with us at service@3P-instruments.com

Figure 2 *Gerd Scharschuh with a part of his farewell gift handed over by the CEO Dr. Dietmar Klank*

Figure 3 *Gerd Scharschuh (left) hands over management of the Service department to Peter Macht (right) with a handshake*

Over 30 years of expertise

Own research and development department

Efficient workflow, very short reaction times

Experienced service team with direct access to test equipment

Lab for Scientific Particle Analyses for test and contract analyses

Possibility of instrument rental and leasing

3P Instruments GmbH & Co. KG
Rudolf-Diesel-Straße 12
85235 Odelzhausen | Germany
Tel. +49 8134 9324 0
info@3P-instruments.com

www.3P-instruments.com

@3P_Instruments
3P-Instruments

ISSN 2750-7084 (Print)
ISSN 2750-7092 (Online)